NASA CR-179632

National Aeronautics and
Space Administration

BLADE LOSS TRANSIENT DYNAMICS ANALYSIS

Final Report
Volume I
TASK II - TETRA 2 THEORETICAL DEVELOPMENT

November 1986

by

Vincente C. Gallardo
Gerald Black

General Electric Company
Aircrafrt Engine Business Group
Cincinnati, Ohio 45215

Prepared For

National Aeronautics and Space Administration

NASA Lewis Research Center
Contract NAS3-24381

1. Report No.	2. Government Accession No.	3. Recipient's Catalog No.

4. Title and Subtitle	5. Report Date
NASA BLADE LOSS PROGRAM TURBINE ENGINE STEADY STATE RESPONSE ANALYSIS VOLUME 1: TETRA 2 THEORETICAL DEVELOPMENT	November 1986
	6. Performing Organization Code
7. Author(s) Vincente C. Gallardo Gerald R. Black	8. Performing Organization Report No.
	10. Work Unit No.
9. Performing Organization Name and Address General Electric Company Aircraft Engine Group 1 Neuman Way Cincinnati, Ohio 45215	11. Contract or Grant No. NAS3-24381
	13. Type of Report and Period Covered Contract Final
12. Sponsoring Agency Name and Address NASA - Lewis Research Center Materials, Structure, and Grants Section 21000 Brook Park Road Cleveland, Ohio 44135	14. Sponsoring Agency Code
15. Supplementary Notes	

16. Abstract

This volume is the documentation of the theoretical development of the forced steady state analysis of the structural dynamic response of a turbine engine having nonlinear connecting elements. Based on Modal synthesis, and the principle of harmonic balance, the governing relations are the compatibility of displacements at the nonlinear connecting elements. There are four displacement compatibility equations at each nonlinear connection, which are solved by iteration for the principal harmonic of the excitation frequency.

The resulting computer program, TETRA 2, combines the original TETRA transient analysis (with flexible bladed disk) with the steady state capability. A more versatile nonlinear rub or bearing element which contains a hardening (or softening) spring, with or without deadband, is also incorporated.

17. Key Words (Suggested by Author(s))	18. Distribution Statement
TETRA, Rotor Dynamics, Turbine Engine, Transient Response, Steady State, Harmonic Balance; Unbalance, Forced Vibration, Blade Out	

19. Security Classif. (of this report)	20. Security Classif. (of this page)	21. No. of Pages	22. Price*
Unc.	Unc.		

TABLE OF CONTENTS

TABLE OF CONTENTS (CONT.)

TABLE OF CONTENTS (CONT.)

ABSTRACT

This volume is the documentation of the theoretical development of the forced steady state analysis of the structural dynamic response of a turbine engine having nonlinear connecting elements. Based on modal synthesis, and the principle of harmonic balance, the governing relations are the compatibility of displacements at the nonlinear connecting elements. There are four displacement compatibility equations at each nonlinear connection, which are solved by iteration for the principal harmonic of the excitation frequency.

The resulting computer program, TETRA 2, combines the original TETRA transient analysis (with flexible bladed disk) with the steady state capability. A more versatile nonlinear rub or bearing element which contains a hardening (or softening) spring, with or without deadband, is also incorporated.

1.0 SUMMARY

The NASA-Lewis Blade Loss program which was originally written for the calculation of transient response of turbine engine structures, has been extended to predict steady state vibratory response. The original name of TETRA (Turbine Engine Transient Response Analysis) has been kept, but slightly modified to TETRA 2. This new program can be used to calculate transient and forced steady state responses. The 'transient' capability is based on the latest version of TETRA and includes the subsequent additions of:

1) Flexible Bladed Disk module
2) Squeeze Film Bearing Module

The 'steady state' capability includes the original modules with the exception of the squeeze film module. However, the original rub element has been generalized to allow either dead-band or no dead-band, and the rub spring characteristics is a hardening spring and/or a linear spring.

Inputs for transient and steady state are the same except for the obvious differences:

Transient requires 'time-sweep' inputs
Steady state requires 'frequency-sweep' inputs.

The basic theoretical approach for the steady state capability requires the formation of a global matrix equation in terms of the generalized coordinates and nonlinear physical forces. Solution is by harmonic balance and iteration of physical displacements at the nonlinear connecting elements. This solution yields only the first harmonic of the forcing frequency.

2.0 INTRODUCTION

In the NASA-Lewis sponsored Turbine Engine Transient Analysis program (TETRA), a computational tool was developed to predict the transient dynamic response of engineering structures to suddenly applied loads, such as from the loss of a blade (1)*. The capability of this program was further enhance by the addition of two modules: 1) Flexible Bladed Disk (2), and 2) Squeeze Film Bearing (3). The latter was added by Case Western Reserve University under NASA-Lewis sponsorship.

The fundamental technical approach is the method of model synthesis (4), wherein the dynamic response of a complex structure is constructed in terms of the natural modes of its principal structural components. The possible breakdown of a turbine engine into its main components is shown in Figure 1-1. The equations of motion in the modal generalized coordinates are solved numerically by central difference integration in the time domain. This solution has the flexibility to accommodate nonlinearities, such as tip rubs, squeeze films or other nonlinear bearings or connecting elements. Also the gyroscopic coupling between motions in the vertical and horizontal planes of rotating structures is considered for rigid as well as flexible bladed disks. Applications of the TETRA are found in References 1, 2 and 5.

The transient response of a structure is a history of the motion and loads which initially vary non-uniformly in time until a steady state condition is reached. Where damping is low and modal frequencies high, the time steps required to reach steady state can be considerable, for this reason a more direct method to calculated steady state response was undertaken.

Steady state capability allows the calculations of forced response amplitudes as function of excitation frequency so that engine response from a sinusoidal input, such as unbalance, can be obtained over the engine operating speed range. For purely linear systems, the methodology is well established.

However, in the presence of nonlinearities, obtaining the steady state solution is neither simple nor straight-forward. This is especially true with large systems of equations with strong nonlinearities. To date, there is no mathematical method to solve the general nonlinear differential equations, (6), (7) and (8).

*Numbers in parentheses indicate references.

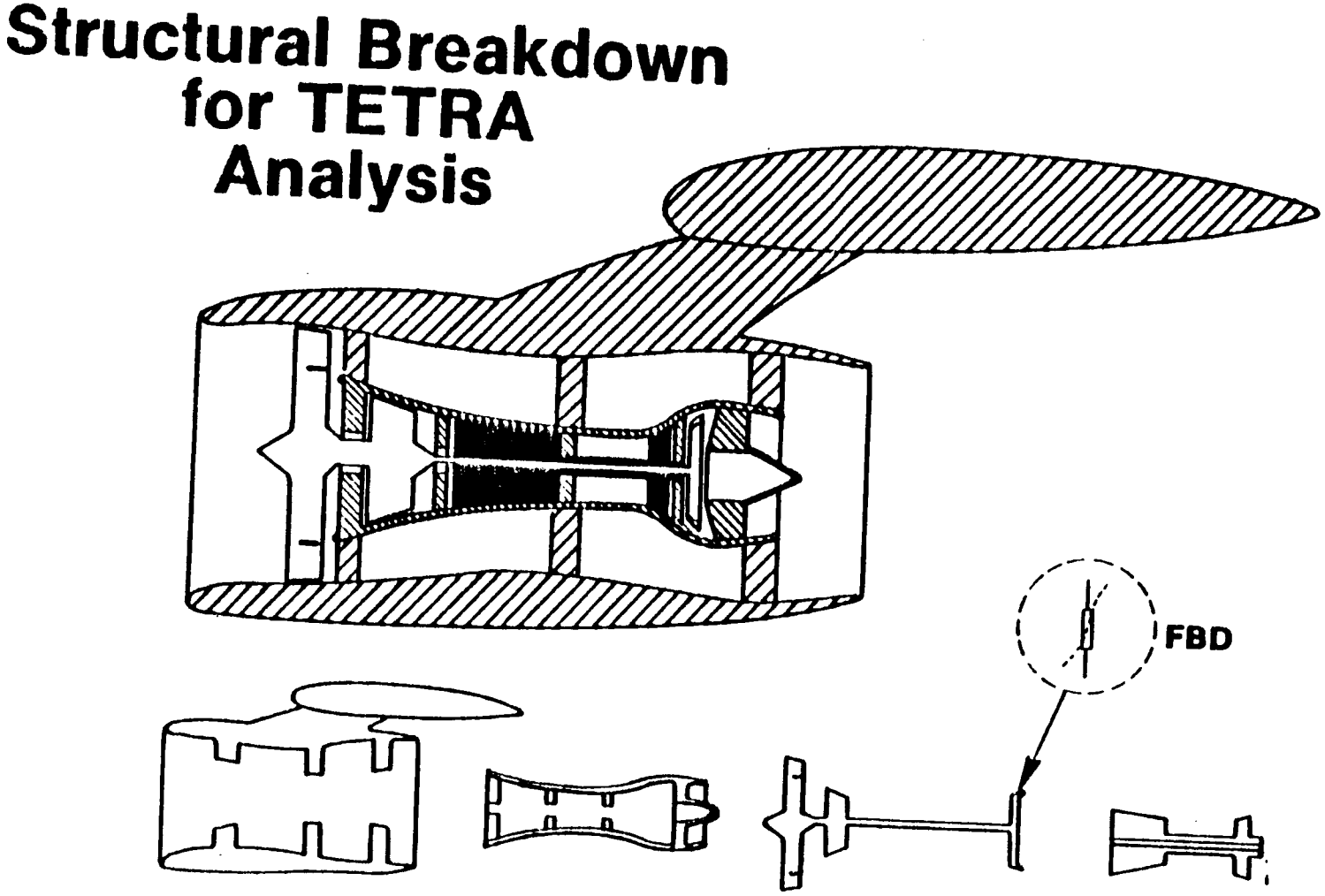

Figure 1-1. Structural Breakdown for TETRA Analysis

To produce a more pragmatic solution to this complex and important problem, the solution is limited to the first harmonic of the forcing frequency. Solution by iteration of the compatibility conditions at only the nonlinear connecting elements results in a dramatic reduction in the number of equations to be solved. The method of harmonic balance, due to Kryloff and Bogoliuboff (9), was used to transform the nonlinear differential equations to a system of nonlinear connections.

This methodology was implemented in a computer code built on the original TETRA program. The new program, TETRA 2, has the capability of the original transient analysis as well as the steady state solution. To make the TETRA 2 user friendly, the inputs of the original TETRA has been kept unchanged as much as possible. The only major addition lies in the description of the 'time-sweep' of the transient analysis and the 'frequency-sweep' of the steady state. The basic description of the structural subsystems and their modal data, the concatenation or assemblage of the subsystems and the connecting elements are essentially the same.

This final report is the documentation of the development of TETRA 2, in particular, the steady state capability. This report consists of two volumes: 1) theory, and 2) user's manual. The latter includes the entire input sheets for the TETRA 2 code: transient and steady state, as well as sample cases, and comparisons of results made for the original two subsystem demonstration cases.

With the NASA sponsored TETRA 2 computer code, industry is presented a comprehensive turbine engine rotor dynamics computer code that can be used for the calculation of both transient and steady state responses. The nonlinear capability of the program greatly enhances and broadens its application to more realistic analysis of real engines.

The authors wish to acknowledge the technical help provided by their colleagues. Dr. J. K. Casey contributed his mathematical expertise in the computational strategy employed in the program, while M. J. Stallone provided overall technical guidance, especially insisting in making TETRA 2 inputs and outputs as similar as possible to the original transient version. Also, we recognize A. Storace for contribution in the overall program and R. Holt for writing the model program that checked out TETRA 2. Finally, to Jeanette Sturgill for a very meticulous and neat typing of the working equations; many thanks.

To our colleagues at NASA-Lewis, thanks to Gerry Brown who managed the original TETRA and Bob Kielb who succeeded him in TETRA 2 and Chuck Lawrence, NASA-Lewis' monitor for the program. We would like to recognize the thorough critical evaluations that the first project monitor of the NASA Blade Loss Program, Ming Tang, has made to TETRA and for the subsequent definition of the early stages of TETRA 2. He has since passed away last year. His thoroughness in reviewing the technical documentations of the Blade Loss Program as well as the very cogent constructive criticisms he provided, have proven invaluable.

3.0 PART I: ANALYTICAL DEVELOPMENT

3.1 Technical Approach to Steady State Response Analysis

The steady state response of systems with nonlinearities is a relatively undeveloped field unlike purely linear systems. Nonlinear differential equations have many possible solutions, each being highly sensitive to initial conditions, external forces and system parameters. For instance, in the case of Duffing's or van der Pol's equation, grossly different solutions are produced by changes in initial conditions or force amplitudes. One initial condition may result in periodic solutions; another may result in aperiodic solutions; still others may yield jumps or bi-stable solutions, limit cycles, and subharmonic and superharmonic oscillations.

When one considers a complex turbine engine with many degrees of freedom and several nonlinearities, the problem of finding general steady state solutions is considerable. In most cases, only approximate solutions with narrow constraints are practicable. In the present work, a pragmatic philosophy is employed which will limit solutions to the first harmonic of the excitation frequency and simple harmonic oscillations with constant amplitude. This is justified from most engine experience, where engine response is essentially in the excitation frequency.

The use of modal synthesis on a large system also limits nonlinearities to inter-subsystem connecting elements, such that the deflection of a structural subsystem can be represented by a superposition of its normal modes. The nonlinear connecting forces are written as function of the relative physical displacements between the joined components and are treated as quasi-external forces. By multiplying these connecting physical forces by the appropriate modal displacements, the global equations in the generalized modal coordinates of the complete assembled structure are obtained.

The left-hand side of the global matrix differential equation contain the linear part which are proportional to the generalized coordinates. On the right-hand side are the generalized forces which are functions of time in the case of external forces, and the nonlinear connecting forces which are explicit functions of the relative physical displacements.

Employing the principles of 'harmonic averaging' or 'harmonic balance' due to Kryloff and Bogoliuboff (9,10) and slowly varying functions (10), the differential equations are transformed to nonlinear algebraic equations. After solving explicitly (by inversion) for the generalized coordinates, the relative physical displacements at the nonlinear connections are obtained by modal superposition. These last equations relate the vector of relative physical displacements at the nonlinear connections on the left-hand side to the external and nonlinear connecting physical forces (in terms of relative physical displacements) on the right-hand side. Thus, the equations to be solved are reduced from twice the number of generalized coordinates to just four times the number of nonlinear connecting elements, which is a considerable reduction.

Numerical solution by iteration of these compatibility relations is made with existing computer subroutines such as those in the IMSL library.

The following sub-sections delineate the technical approach described here, in more technical details.

3.1.1 Generalized Global Equations of Structural Systems With Nonlinear Connecting Elements

Following the method of modal synthesis, the global equations of motion of a system of inter-connected elastic bodies were derived in Reference 1,2, and 4. Those obtained in (1) and (2) were solved in the transient TETRA and are the same ones solved in TETRA 2. To illustrate the basic concept of the method employed in the steady state analysis, the denotation of each structural component and plane(s) (horizontal and vertical planes) will be omitted for simplicity. A very detailed development of the working equations actually programmed, is presented in a later section.

Conceptually, the equations of motion of the fully coupled and assembled system are written in tensor (or matrix) notation. The dependent variables, $q_i(t)$ are the generalized modal coordinates of the component structures. Since each component structure's normal modes are obtained with free-free boundary conditions, these satisfy orthogonality only within the individual structures, such that coupling forces between substructures and their normal modes exist. In short, the matrices of the coefficients of the generalized modal coordinates are not diagonal, but in general, full matrices.

The generalized nonlinear connecting forces are functions of the relative physical displacements between the joined structures at the connected points. Though these displacements belong to a subset of the physical displacements of the substructures, these 'connection' displacements are not expressed in terms of normal modes. Thus, the nonlinear connecting forces are always in terms of the relative physical displacements.

From (1) and (2), the global equations of motion in the generalized coordinates are given in tensor form as:

$$M_{ij}\ddot{q}_j + \left\{\omega_{ij}^2 M_{ij} + \sum_n K_{ij}^n\right\} q_j + \left\{2\zeta_{ij}\omega_{ij}M_{ij} + \sum_n C_{ij}^n + \Omega G_{ij}\right\}\dot{q}_j = F_i(t) + H_i(\Delta X^m)$$

Where:

M_{ij}= modal mass matrix (non-diagonal with the flexible bladed disk module)

ω_{ij} = modal natural frequencies, diagonal matrix

ζ_{ij} = modal critical damping ratio

G_{ij}= gyro coupling - skew symmetric matrix

n = axial location of linear connecting element

K_{ij}^{n} = generalized linear connecting spring matrix, summed over the 'n' linear connections

C_{ij}^{n}=generalized linear damping matrix associated with K_{ij}^{n}

$F_i(t)$- generalized external force - sinusoidal

$H_i(\Delta X^m)$ = modal nonlinear connecting forces at m locations. Summed over m locations.

ΔX^m = Relative physical displacement at the nonlinear connecting element with axial location m.

The generalized nonlinear connecting forces are given as a hardening spring with viscous damping, and written in terms of the physical displacements. For example, one nonlinear spring force at point 'm' is given as a physical force:

$$F^m = -K^m[1 + \mu^m(\Delta X^m)^2]\Delta X^m - C^m\Delta\dot{X}^m$$

Where: K^m= the linear part of the spring

μ^m= the nonlinear factor

X^m= the relative physical displacement at location 'm'

C^m= viscous damping coefficient of the connecting element.

The generalized nonlinear connecting force on a subsystem at point 'm' is simply the product of the physical force F^m times the subsystem's modal displacement at point 'm' in the i^{th} mode; thus:

$$\Phi_i^m F^m = -\Phi_i^m\left[K^m\left\{1 + \mu^m(\Delta X^m)^2\right\}\Delta X^m + C^m\Delta\dot{X}^m\right]$$

Where:

$$\Phi_i^m = i^{th}\ mode\ displacement\ at\ \ point\ 'm'$$

When there is more than one nonlinear connection, the physical connecting forces are multiplied by the modal displacements at their locations and summed over those locations - for each mode. The i^{th} generalized nonlinear connecting force is therefore:

$$H_i = -\sum_m \Phi_i^m F^m = -\sum_m \Phi_i^m \left\{ k^m \left(1 + \mu^m \left[\Delta x^m \right]^2 \right) \right\} - \sum_m \Phi_i^m C^m \Delta \dot{X}^m$$

The global generalized equations may therefore be rewritten:

$$\Psi_i = M_{ij} \ddot{q}_j + \left\{ \omega^2_{(ij)} M_{ij} + \sum_n K_{ij}^n \right\} q_j + \left\{ 2\omega_{(ij)} \zeta_{(ij)} M_{ij} + \sum_n C_{ij}^n + \Omega G_{ij} \right\} \dot{q}_j$$

$$-F_i - \sum_m \Phi_i^m K^m \left\{ 1 + \mu^m [\Delta X^m]^2 \right\} \Delta X^m - \sum_m \Phi_i^m C^m \Delta \dot{X}^m = 0$$

3.1.2 Transformation by Harmonic Balance and the Compatibility Relations

The global generalized differential equations are nonlinear in the physical displacements at the nonlinear connecting elements. To obtain forced solutions synchronous with the excitation frequency, an assumption of slowly varying function is made. This assumes that the principal motion is harmonic with constant amplitude, so that the ensuing generalized - and physical - displacements, may be written in the form:

$$q_i(t) = a_i \cos\omega t + b_i \sin\omega t$$

$$X^m(t) = A^m \cos\omega t + B^m \sin\omega t$$

with $$\dot{a}_i = \dot{b}_i = \dot{A}^m = \dot{B}^m = \ddot{a}_i = \ddot{b}_i = \ddot{A}^m = \ddot{B}^m = 0$$

The next step is to employ the principle of harmonic balance (9,10,11) by means of which the "N" differential equations are transformed to "2N" nonlinear algebraic equations.*

The transformation is made as follows: Substitute the harmonic form of the displacements into the N global generalized differential equations; multiply each equation by $'\cos\omega t\, dt'$ and integrate from 0 to $2\pi/\omega$; repeat the last step but multiply with $'Sin\omega t\, dt'$ and integrate as before.

Recalling that each global generalized equation is identified as: $\Psi_i = 0$, the transformation becomes:

$$\begin{pmatrix} \bar{\Psi}_i^c \\ \bar{\Psi}_i^s \end{pmatrix} = \int_0^{2\pi/\omega} \Psi_i \left(a_i b_i A^m B^m \omega t \ldots \right) \begin{pmatrix} \cos\omega t \\ \sin\omega t \end{pmatrix} dt = 0$$

Where: Ψ_i^c = cosine transformation

Ψ_i^s = sine transformation

*2N, when motions are in only one plane; 4N when motions are in 2 planes.

The following integral transformations, which are inferred from the terms of the global generalized differential equations, are required:

$$\frac{\omega}{\pi}\int_{t=0}^{2\pi/\omega} \ddot{q}_i \begin{pmatrix} cos\omega t \\ sin\omega t \end{pmatrix} dt = \begin{pmatrix} -\omega^2 a_i \\ -\omega^2 b_i \end{pmatrix}$$

$$\frac{\omega}{\pi}\int_{t=0}^{2\pi/\omega} \dot{q}_i \begin{pmatrix} cos\omega t \\ sin\omega t \end{pmatrix} dt = \begin{pmatrix} \omega b_i \\ -\omega a_i \end{pmatrix}$$

$$\frac{\omega}{\pi}\int_{t=0}^{2\pi/\omega} q_i \begin{pmatrix} cos\omega t \\ sin\omega t \end{pmatrix} dt = \begin{pmatrix} a_i \\ b_i \end{pmatrix}$$

$$\frac{\omega}{\pi}\int_{t=0}^{2\pi/\omega} X^m \begin{pmatrix} cos\omega t \\ sin\omega t \end{pmatrix} dt = \begin{pmatrix} A^m \\ B^m \end{pmatrix}$$

$$\frac{\omega}{\pi}\int_{t=0}^{2\pi/\omega} \dot{X}^m \begin{pmatrix} cos\omega t \\ sin\omega t \end{pmatrix} dt = \begin{pmatrix} \omega B^m \\ -\omega A^m \end{pmatrix}$$

$$\frac{\omega}{\pi}\int_{t=0}^{2\pi/\omega} [X^m]^3 \begin{pmatrix} cos\omega t \\ sin\omega t \end{pmatrix} dt = \begin{pmatrix} \frac{3}{4} A^m \left[(A^m)^2 + (B^m)^2 \right] \\ \frac{3}{4} B^m \left[(A^m)^2 + (B^m)^2 \right] \end{pmatrix}$$

Where:

$$q_i = a_i cos\omega t + b_i sin\omega t$$

$$X^m = A^m cos\omega t + B^m sin\omega t$$

With these transformations, the differential equations become algebraic equations. Thus,

$$\begin{bmatrix} AA_{ij} & AB_{ij} \\ BA_{ij} & BB_{ij} \end{bmatrix} \begin{pmatrix} a_i \\ b_i \end{pmatrix} = \begin{pmatrix} F_i^c \\ F_i^s \end{pmatrix} + \begin{bmatrix} \overline{H}_i^c \left\{ \sum \left(\Delta A^m, \Delta B^m \ldots \right) \right\} \\ \overline{H}_i^s \left\{ \sum \left(\Delta A^m, \Delta B^m \ldots \right) \right\} \end{bmatrix}; \; i,j: 1,2 \ldots N$$

Where: AA_{ij}, AB_{ij}, BA_{ij}, BB_{ij} are the coefficients of the generalized coordinates

F_i^c = cosine transformation of the external general force

F_i^s = Sine transformation of the external general force

$\overline{H}_i^c$ = Cosine transformation of the nonlinear connecting force, a function of the A^m, B^m components at <u>all</u> nonlinear connecting elements. This may be a polynomial in A^m, B^m of the form: $\left(A^1\right)^3, \left(B^1\right)^3; \left(A^1\right)\left(A^1\right)^2;$ *etc.*

Where m: $1,2,\ldots M$

$\overline{H}_i^s$ = Same as $\overline{H}_i^c$, except it is for the Sine transformation.

The previous transformed matrix equation may be written more simply with a change in the range of the index i:

$$E_{ij} \alpha_j = F_i + \overline{H}_i \left\{ \sum \left(\Delta A^m, \Delta B^m \ldots \right) \right\}$$

Where $i,j = 1,2,\ldots 2N$

$\alpha_j = a_j$, $i = 1,2,\ldots N$

$\alpha_j = b_j$, $i = N+1, N+2, \ldots 2N$

$E_{ij} = \left[AA_{ij} \ldots \right]$

Inverting the Eij matrix, one obtains an explicit expression for the generalized coordinates:

$$\alpha_i = a_1, a_2 \ldots a_n; \; b_1, b_2 \ldots b_n$$

$$\alpha_i = E_{ij}^{-1} F_j + E_{ij}^{-1} \overline{H}_j \left\{ \sum \left(\Delta A^m, \Delta B^m \ldots \right) \right\}; \; \textit{repeated index } j \textit{ denotes summation}$$

The first term on the right-hand side is the vector of generalized displacements due to the external forces alone, while the second are due to the unknown physical displacements at nonlinear elements.

Thus there are 2N equations with 2N + 2M unknowns; the latter being the cosine (A^m) and Sine (B^m) components of the relative physical displacements at M nonlinear connections. These are the ultimate unknowns. To solve for the A^m and B^m's, displacement compatibility relations at the nonlinear connections are formed.

Recall that: $X^m = \phi_i^m q_i$

From the assumed harmonic form of the displacements, it follows that at point m:

$$A^m = \phi_i^m a_i = \sum_{i=1}^{N} \phi_i^m a_i = \sum_{i=1}^{N} \Phi_i^m \alpha_i$$

$$B^m = \phi_i^m b_i = \sum_{i=1}^{n} \phi_i^m b_i = \sum_{i=N+1}^{2N} \Phi_i^m \alpha_i$$

where the repeated index i indicates summation over the modes.

The components of the physical displacements at any of the nonlinear elements are therefore:

$$A^m = \sum_{i=1}^{N} \Phi_i^m \alpha_i = \sum_{i=1}^{n} \Phi_i^m \left[\sum_{j=1}^{N} \left\{ E_{ij}^{-1} F_j + E_{ij}^{-1} \overline{H}_j \left(\sum_l \Delta A^l, \Delta B^l \ldots \right) \right\} \right]$$

$$B^m = \sum_{i=N+1}^{2N} \Phi_i^m \alpha_i = \sum_{i=N+1}^{2n} \phi_i^m \left[\sum_{j=N+1}^{2N} \left\{ E_{ij}^{-1} F_j + E_{ij}^{-1} \overline{H}_j \left(\sum_l \Delta A^l, \Delta B^l \ldots \right) \right\} \right]$$

NOTE:

$$\Phi_i^m \Big|_{i=1}^{N} = \Phi_i^m \Big|_{i=N+1}^{2N}$$

Forming similar physical displacements at both ends of a nonlinear connecting element, one obtains their difference which is the relative physical displacement. Thus, for the cosine component at point m:

$$\textcircled{1} A^m - \textcircled{2} A^m = \Delta A^m = < \sum_{i=1}^{N} \Phi_i^m \left[\sum_{j=1}^{N} \left\{ E_{ij}^{-1} F_j + E_{ij}^{-1} \overline{H}_j \left(\sum_l \Delta A^l, \Delta B^l \ldots \right) \right\} \right] >_{\textcircled{1}}$$

$$- < \sum_{i=1}^{N} \Phi_i^m \left[\sum_{j=1}^{N} \left\{ E_{ij}^{-1} F_j + E_{ij}^{-1} \overline{H}_j \left(\sum_l \Delta A^l, \Delta B^l \ldots \right) \right\} \right] >_{\textcircled{2}}$$

A similar expression is obtained for the Sine component:

$$①B^m - ②B^m = \Delta B^m$$

In like manner, relative physical displacements at all the nonlinear connecting elements are obtained, resulting in compatibility relations or iterating equations whose number is twice the number of nonlinear elements. By this process we have reduced the number of iterating equations from 2N (twice the number of generalized modal coordinates) to 2M (twice the number of nonlinear connecting elements).

Substituting the relative physical displacements (obtained by iteration) into the explicit expressions for the generalized coordinates, one then obtains the complete solution. The physical displacement at any point on any physical subsystem is calculated by simple superposition.

The previous discussion tacitly assumed that the nonlinear connecting elements were planar. However, nonlinear rotor bearings deflect in a radial direction. This has components in both vertical and horizontal planes. With this regard, the displacement compatibility relations must be found in 2 planes, which increases the number of iterating equations to 4M (four times the number of nonlinear elements) - still a considerable reduction from two times the number of generalized coordinates. Note that the generalized modal coordinates include vertical as well as horizontal degrees of freedom.

It will be noted that the global matrix equation of motion as well as the compatibility relations at nonlinear connections are derived in the standard way: by Lagrangian or Newtonian formulation and modal superposition. No recourse to Lagrangian multipliers was made to obtain the compatibility equations via constraint relations, as was done in (11). This theoretical rationalization helps establish the fundamental basis for the methodology. However, the results obtained in the present work by the standard formulation are identical to what would be derived with the concept of Lagrangian multipliers (11).

3.2 Application to Turbine Engine Steady State Response

The preceding theoretical approach was applied to the turbine engine problem employing the earlier formulation of TETRA. Thus the reconstruction of the entire engine's dynamic response from the modal characteristics of its components' normal modes is made by modal synthesis. The modeling of the engine structure is unchanged.

However, rather than selecting the time history of the engine response (for the transient case), one picks the range of frequencies where the solution is required in the steady state analysis.

Because the general rub or bearing element (nonlinear spring) produces a force that is a cubic in the relative displacement, the radial nature of the displacements means that the connecting forces couple motions in the horizontal and vertical planes. Thus the components of the forces and physical displacements at the nonlinear connections are four in number:

(1) Vertical
(2) Horizontal
(3) Cosine Component
(4) Sine Component

This means that the number of iterating or compatibility relations is four times the number of nonlinear connecting elements rather than the two times in a system of a single plane.

3.3 Solution of the Compatibility Relations

The reduced algebraic equations governing displacement compatibility at nonlinear connecting elements is equal in number to 4-times the number of nonlinear connections. Principal unknowns are the relative physical displacements at these junctures. This system of nonlinear simultaneous equations are solved by iteration. Because of the doubly nonlinear character of the general rub element, the convergence of the iteration routine may not always be certain. The double nonlinearity arises from this, that the rub (or nonlinear) element has both a cubic term and a deadband. The deadband itself is a nonlinear property even when the associated spring rates are constant. However, the convergence problem is not really serious when deflections are small (in the order of bearing clearances). Only when deflections are very large will these problems arise.

In the computational algorithm developed for TETRA 2, the iteration subroutine is written as a module which may be replaced or added to - at the option of the user. The program has 2 IMSL iteration modules. These are based on Newton's Method and the Secant Method.

The relative physical displacements, determined by iteration, allow calculating all the forces in the system of equations in the generalized coordinates, and hence, all the modal amplitudes. The latter is performed simply by inversion technique. Subsequently, the physical displacements at all points in the complete structure are found by superposition. These, as well as the bearing loads, are found as in the original TETRA.

The following sections are the amplification and application of the basic theory to the detailed analysis of the TETRA engine model. These contain the explicit and very detailed working relations describing the global matrix differential equation formation, the transformation to algebraic equations by harmonic balance, formulation of the iterating equations and the special treatment of the deadband. The latter describes the numerical procedure for performing the harmonic balance when rubbing is intermittent rather than continuous.

In the next volume, which is also the user's manual, sample cases are described along with input and output descriptions. Because TETRA 2 replaces the original TETRA program, with the dual capability of transient and steady state analyses, the full and complete set of input sheets (with descriptions and instructions) and output options are given.

4.0 Part II: Detailed Application of the Theory to Turbine Engines

The turbine engine modeling developed in the original TETRA has been presented, e.g., the ordered concatenation of the structural subsystems in terms of their normal modes and as governed by the method of modal synthesis. However, for the steady state cases the equations to be solved are the displacement compatibility relations at the nonlinear connections, which number four at each of these joints.

As discussed in Part I, the steady State response analysis requires the following:

1) Formation of a global matrix differential equation in the generalized coordinates

2) Transformation of these equations by the principle of harmonic balance with simultaneous nonlinear algebraic equations

3) Formation of displacement compatibility relations at nonlinear connecting elements

4) Iterative solution of the compatibility relations - yielding the relative physical displacements at the nonlinear connections

5) Substitution of these physical displacements in the transformed global equations of the generalized coordinates, and calculating the latter by inversion

6) Calculating the physical response of the entire engine by superposition

These calculations were made in the frequency domain so that the results describe the forced steady state response of a turbine engine at the principal harmonic of the excitation frequency.

The implementation of the methodology in the original TETRA program has resulted in TETRA 2, which now has the dual capability of the transient version and steady state. In addition, the scope of the transient version has been increased to contain the following enhancements initially developed for the steady state analysis: improved rub element (with the cubic nonlinear factor), structural damping capability (applies for physical connecting element types 1, 2, 4, and 5), and new printout options.

Because the transient analysis has been virtually untouched, this portion of the report is concerned only with theoretical details of the steady state analysis. Only in the user's manual, (Volume 2) are the transient and steady state options merged together via input sheets and output.

The following sections document the detailed working equations and their implementation into TETRA 2. One should use the fundamental global matrix differential equations presented in Part I as a general reference in reading what follows, because this provides a bird's eye view of the equations to be solved and the inter-relationships of the various elements. For instance, it should be noted that forces are initially derived in physical space and subsequently developed in generalized coordinate space. This is followed for flexible bladed disk, gyro linear connecting elements, and nonlinear connections.

4.1 Applied Forces For a Steady State Analysis

4.1.1 Physical Unbalance Forces

The unbalance forces are illustrated in the figure on the type K-1 input sheet. Only the steady state unbalance forces are discussed here, since the transient analysis unbalance loads were covered in reference 1. For a steady state run, the unbalance forces are:

$$F_{ujz} = U\omega^2 sin(\omega t + \phi)$$

$$F_{ujy} = U\omega^2 cos(\omega t + \phi)$$

where:

F_{ujz} = Unbalance load at point j in the z (vertical) direction.

F_{ujy} = Unbalance load at point j in the y (horizontal) direction.

ω = rotor speed
t = time
U = unbalance magnitude for the unbalance load
ϕ = Phase angle for the unbalance load

Note: For each unbalance load the global point number j, unbalance magnitude U , and phase angle Φ is input (see type K-2 namelist input sheet). More than one unbalance load may be inputted for a given point.

Using trigonometric identities, we can rewrite the unbalance forces in terms of cos and sin components as follows:

$$F_{ujz} = U\omega^2 sin\,\phi\, cos\,\omega t + U\omega^2 cos\,\phi\, sin\,\omega t$$
$$F_{ujy} = U\omega^2 cos\,\phi\, cos\,\omega t - U\omega^2 sin\,\phi\, sin\,\omega t$$

Letting

$$F_{ujz} = F^c_{ujz} cos\,\omega t + F^s_{ujz} sin\,\omega t$$
$$F_{ujy} = F^c_{ujy} cos\,\omega t + F^s_{ujy} sin\,\omega t$$

we see that the magnitudes of the cos and sin components are:

$$F^c_{ujz} = U\omega^2 sin\,\phi$$

$$F^s_{ujz} = U\omega^2 cos\,\phi$$

$$F^c_{ujy} = U\omega^2 cos\,\phi$$

$$F^s_{ujy} = -U\omega^2 sin\,\phi$$

4.1.2 Physical Pcos $(\omega t + \Phi)$ Forces

For a steady state analysis run, TETRA 2 also makes provision for inputting applied loads of the form:

$$F_{pjk} = P\cos(\omega t + \phi)$$

where:

F_{pjk} = Applied forces at global point j in global direction k.

P = Force magnitude for the load
ω = Steady state forcing frequency
t = Time
ϕ = Phase angle for the load

Note: For each Pcos $(\omega t + \phi)$ load, the global point number j, force magnitude P, phase angle Φ , and global direction number k is inputted (see type L-2 input sheet).

Using a trigonometric identity we have:

$$F_{pjk} = P\cos\phi\cos\omega t - P\sin\phi\sin\omega t$$

Letting

$$F_{pjk} = F^c_{pjk}\cos\omega t + F^s_{pjk}\sin\omega t$$

we see that the magnitudes of the cos and sin components of the force are:

$$F^c_{pjk} = P\cos\Phi$$

$$F^s_{pjk} = -P\sin\Phi$$

4.1.3 Total Physical Applied Forces

The total applied force for a given point and direction can be written in terms of the cos and sin components as follows:

$$F_{ajk} = F^c_{ajk}\cos\omega t + F^s_{ajk}\sin\omega t$$

where:

F_{ajk} = Total applied force for global point j and global direction k

F^c_{ajk} and F^s_{ajk} are obtained by summing the unbalance loads and the $P\cos(\omega t + \Phi)$ loads for global point j and global direction k as follows:

$$F^c_{ajk} = \sum F^c_{ujk} + \sum F^c_{pjk} \qquad F^s_{ajk} = \sum F^s_{ujk} + F^s_{pjk}$$

where

F^c_{ujk} = Magnitude of the cos component of an input unbalance load for global point j and global direction k (see section 4.1.1)

F^s_{ujk} = Magnitude of the sin component of an input unbalance load for global point j and global direction k (see section 4.1.1)

F^c_{pjk} = Magnitude of the cos component of an input $P\cos(\omega t + \phi)$ load for global point j and global direction k (see section 4.1.2)

F^s_{pjk} = Magnitude of the sin component of an input $P\cos(\omega t + \phi)$ load for global point j and global direction k (see section 4.1.2)

4.1.4 Generalized Applied Forces

The generalized force for generalized coordinate i may be written in terms of the cos and sin components as follows:

$$F_i = F^c_i \cos\omega t + F^s_i \sin\omega t$$

where:

F_i = Generalized force for generalized coordinate (global mode) i

$$F^c_i = \sum_{j=1}^{n}\sum_{k=1}^{6} F^c_{ajk}\,\Phi_{ijk}$$

$$F^s_i = \sum_{j=1}^{n}\sum_{k=1}^{6} F^s_{ajk}\,\Phi_{ijk}$$

where

F^c_{ajk} = Magnitude of the cos component of the total applied force for global point j and global direction k (see section 4.1.3)

F^s_{ajk} = Magnitude of the sin component of the total applied force for global point j and global direction k (see section 4.1.3)

Φ_{ijk} = Mode shape for global mode i, global point j, and global direction k

4.2 Linear Physical Connecting Elements

There are six types of physical connecting elements. All of the six types can be used for either transient analysis or steady state analysis runs with the exception of the type 6 element (squeeze film damper element), which can be used for transient analysis runs only. The linear physical connecting elements include type 1 (general spring - damper element), type 2, (link - damper element), type 4 (engine support - links element), and type 5 (uncoupled point spring - damper element). This section discusses the equations used for the linear (types 1,2,4, and 5) physical connecting elements for a steady state analysis run. The equations used for the nonlinear type 3 element (rub element) for a steady state analysis run will be discussed in section 5.

4.2.1 Transformation Matrix

For steady state analysis runs, a transformation matrix [Φ] must be calculated for each of the linear (type 1,2,4 or 5) physical connecting elements to aid in calculating the contributions of the element to the global matrices.

A sample transformation matrix is shown in figure 4-1. This figure shows the transformation matrix for element 3 of the demonstrator model. For this element, joint I (global point number 5) lies on the rotor (consisting of modal subsystems 1 and 2) and joint J (global point number 2) lies on the case (consisting of modal subsystems 7 and 8). Modal subsystem 1 (the vertical plane subsystem) has 5 modes (global modes 1 through 5), modal subsystem 2 has 5 modes (global modes 6 through 10), modal subsystem 7 has 3 modes (global modes 11 through 13), and modal subsystem 8 has 3 modes (global modes 14 through 16). The transformation matrix simply consists of the mode shapes filled in at the appropriate positions, and the remainder (the bulk of the matrix) filled with zeroes.

Figure 4-1. Sample Physical Connecting Element Transformation Matrix $[\Phi]$

$[\Phi] =$

ELEMENT DIRECTION		GLOBAL MODE NUMBER															
		1	2	3	4	5	6	7	8	9	10	11	12	13	14	15	16
1	z	$\Phi_{1,I,1}$	$\Phi_{2,I,1}$	$\Phi_{3,I,1}$	$\Phi_{4,I,1}$	$\Phi_{5,I,1}$	0	0	0	0	0						
2	θ_y	$\Phi_{1,I,2}$	$\Phi_{2,I,2}$	$\Phi_{3,I,2}$	$\Phi_{4,I,2}$	$\Phi_{5,I,2}$	0	0	0	0	0						
3	y	0	0	0	0	0	$\Phi_{6,I,3}$	$\Phi_{7,I,3}$	$\Phi_{8,I,3}$	$\Phi_{9,I,3}$	$\Phi_{10,I,3}$			0			
4	θ_z	0	0	0	0	0	$\Phi_{6,I,4}$	$\Phi_{7,I,4}$	$\Phi_{8,I,4}$	$\Phi_{9,I,4}$	$\Phi_{10,I,4}$						
5	x	0	0	0	0	0	0	0	0	0	0						
1	z											$\Phi_{11,J,1}$	$\Phi_{12,J,1}$	$\Phi_{13,J,1}$	0	0	0
2	θ_y											$\Phi_{11,J,2}$	$\Phi_{12,J,2}$	$\Phi_{13,J,2}$	0	0	0
3	y						0					0	0	0	$\Phi_{14,J,3}$	$\Phi_{15,J,3}$	$\Phi_{16,J,3}$
4	θ_z											0	0	0	$\Phi_{14,J,4}$	$\Phi_{15,J,4}$	$\Phi_{16,J,4}$
5	x											0	0	0	0	0	0

$\Phi_{i,j,k}$ = *Mode shape for global mode number i, point (joint) j, and element direction k*

4.2.2 Stiffness Contributions

The contributions of a linear (type 1, 2, 4 or 5) physical connecting element to the global stiffness matrix is:

$$[SC] = [\phi]^T [K][\phi]$$

where

$[SC]$ = Stiffness contributions matrix for the element
$[\phi]^T$ = Transpose of the element transformation matrix
$[K]$ = Element stiffness matrix
$[\phi]$ = Element transformation matrix (see section 4.2.1)

[sc] is usually a smaller matrix than the global stiffness matrix, and the terms of the stiffness contributions matrix [sc] must be added into the global stiffness matrix at the appropriate positions.

For a more detailed description of the global stiffness matrix, see section 4.4.3

4.2.3 Damping Contributions

4.2.3.1 Non-Structural Damping

For non-structural damping, the element damping matrix [c] is constant and is not a function of rotor speed or forcing frequency. The element damping matrix [c] for non-structural damping may be defined by input damping matrix definition, or computed from input damping coefficients, or computed using the element stiffness matrix, input element Q factor, and input element selected frequency. In any event, the non-structural damping contributions of a linear (type 1, 2, 4 or 5) physical connecting element to the global velocity matrix is as follows:

$$[NSDC] = [\phi]^T [C][\phi]$$

where:

$[NSDC]$ = Non-structural damping contribution matrix for the element
$[\phi]^T$ = Transpose of the element transformation matrix
$[C]$ = Element damping matrix
$[\phi]$ = Element transformation matrix (see section 4.2.1)

[*NSDC*] is usually a smaller matrix than the global velocity matrix, so the terms of the non-structural damping contributions matrix [*NSDC*] must be added into velocity matrix $[C_0]$ at the appropriate positions. For further details, see section 4.4.4.

4.2.3.2 Structural Damping

For structural damping, the contributions of the element to the global velocity matrix are calculated using the element stiffness matrix [K], input element Q - factor, and either the independent rotor speed (if ISF = 1 on the type A input sheet) or the steady state forcing frequency (if ISF = 2 on the type A input sheet). The structural damping contributions are first collected into a structural damping contributions matrix $[C_S]$ (see section 4.4.4). The contributions of each of the linear (type 1, 2, 4, and 5) physical connecting elements to this structural damping contributions matrix is:

$$[SDC] = \frac{1}{QF}[\Phi]^T [K][\Phi]$$

where:

[SDC] = Structural damping contributions matrix for the element.
QF = Input Q - factor for the element
$[\Phi]^T$ = Transpose of the element transformation matrix
$[K]$ = Element stiffness matrix
$[\Phi]$ = Element transformation matrix (see section 4.2.1)

[SDC] is usually a smaller matrix than the structural damping contributions matrix $[C_S]$, so the terms of [SDC] must be added into $[C_S]$ at the appropriate positions. After the structural damping contributions matrix $[C_S]$ is computed, it must be multiplied by either the reciprocal of the independent rotor speed (if ISF = 1 on the type A input sheet) or the reciprocal of the steady state forcing frequency (if ISF = 2 on the type A namelist input sheet). For more details, see section 4.4.4.

Structural damping is a new feature that has been added to TETRA 2 , and which was not present in the earlier TETRA program. This feature may be used for either steady state or transient analysis runs. Structural damping is applicable for the linear (type 1, 2, 4, or 5) physical connecting elements only.

4.3 Gyroscopic Elements

4.3.1 Transformation Matrix

For steady state analysis runs, a transformation matrix [Φ] must be calculated for each gyroscopic element to aid in calculating the contributions of the element to the global matrices (just as is done for the linear physical connecting elements).

A sample gyroscopic element transformation matrix is shown in figure 4-2. This figure shows the transformation matrix for the gyroscopic element at global point 4 of the demonstrator model. This gyroscopic element lies on rotor 1 (the independent rotor). Rotor 1 consists of modal subsystems 1 and 2. Modal subsystem 1 (the vertical plane subsystem) has 5 modes (global modes 1 through 5), and modal subsystem 2 also has 5 modes (global modes 6 through 10). The transformation matrix simply consists of the applicable mode shapes filled in at the appropriate positions, and the rest of the matrix filled with zeroes.

4.3.2 Velocity Contributions

The gyroscopic element contributions to the global velocity matrix are collected in a gyroscopic contributions matrix for the independent rotor $[G_I]$ and a gyroscopic contributions matrix for the dependent rotor $[G_D]$. The contribution of a gyroscopic element to either the gyroscopic contributions matrix for the independent rotor $[G_I]$ (if the gyroscopic element lies on the independent rotor) or the gyroscopic contributions matrix for the dependent rotor $[G_D]$ (if the gyroscopic element lies on the dependent rotor) is:

$$[GC] = [\phi]^T [G] [\phi]$$

where:

$[GC]$ = Gyroscopic contributions matrix for the gyroscopic element
$[\phi]^T$ = Transpose of the gyroscopic element transformation matrix
$[G] = \begin{bmatrix} 0 & I_p \\ -I_p & 0 \end{bmatrix}$ = Gyroscopic element matrix at point (joint) I on the rotor

I_p = Polar mass moment of inertia at point (joint) I on the rotor
$[\phi]$ = Gyroscopic element transformation matrix (see section 4.3.1)

The gyroscopic contributions matrix for the independent rotor must then be multiplied by the independent rotor speed, and the gyroscopic contributions matrix for the dependent rotor must be multiplied by the dependent rotor speed. See section 4.4.4 for more details.

GLOBAL MODE NUMBER									
1	2	3	4	5	6	7	8	9	10

$$\left[\Phi\right] = \begin{bmatrix} \textit{ELEMENT} \\ \textit{DIRECTION} \end{bmatrix} \begin{matrix} 1 & 0_z \\ 2 & 0_y \end{matrix} \begin{bmatrix} \Phi_{1,I,1} & \Phi_{2,I,1} & \Phi_{3,I,1} & \Phi_{4,I,1} & \Phi_{5,I,1} & 0 & 0 & 0 & 0 & 0 \\ 0 & 0 & 0 & 0 & 0 & \Phi_{6,I,2} & \Phi_{7,I,2} & \Phi_{8,I,2} & \Phi_{9,I,2} & \Phi_{10,I,2} \end{bmatrix}$$

$\Phi_{i,I,k}$ = *Mode shape for global mode number* i, *point (joint)* I, *and element direction* k.

Figure 4-2. Sample Gyroscopic Element Transformation Matrix $\left[\Phi\right]$

4.4 Formation of the Global Matrices

4.4.1 Matrix Equation

The equation of motion is:

$$[M]\ddot{q} + [K]q + [C]\dot{q} = F + H$$

where:

q = generalized displacement
[M] = global mass matrix
[K] = global stiffness matrix
[C] = global velocity matrix
[F] = generalized applied (external) force vector
[H] = generalized nonlinear (rub) element force vector

The following sections detail how we find the [M], [K], and [C] global matrices. In addition, we will also show how we combine the [M], [K], and [C] matrices into one global solution matrix [GM].

4.4.2 Global Mass Matrix [M]

$$\left[M\right] = \left[M\right]_{modal\ masses} + \left[M\right]_{flexible\ bladed\ disks}$$

The global mass matrix consists of the diagonal modal mass terms and the non-diagonal terms due to the flexible bladed disks (if any). These terms are saved in arrays in TETRA. The global mass matrix itself is not saved in TETRA, but rather the terms of the global mass matrix are written directly into the global solution matrix in subroutine GLOB2.

A sample global mass matrix is shown in figure 4-3. This figure shows the global mass matrix for a model consisting of one rotor on which two flexible bladed disks are located. The rotor is composed of two modal subsystems (one for the vertical plane and one for the horizontal plane), and each flexible bladed disk is also itself a modal subsystem, making a total of four modal subsystems.

Note that the steady state analysis global mass has the same format as the flexible bladed disk mass matrix used for a transient analysis run (which is shown on page 70 reference 2). However, the transient analysis flexible bladed disk mass matrix only includes the modes for the rotor on which the flexible bladed disks are located and the modes for the flexible bladed disks, and is only found if at least one flexible bladed disk is present. The steady state global mass matrix, on the other hand, includes all the modes for the model, and is always needed, even if there are no flexible bladed disks.

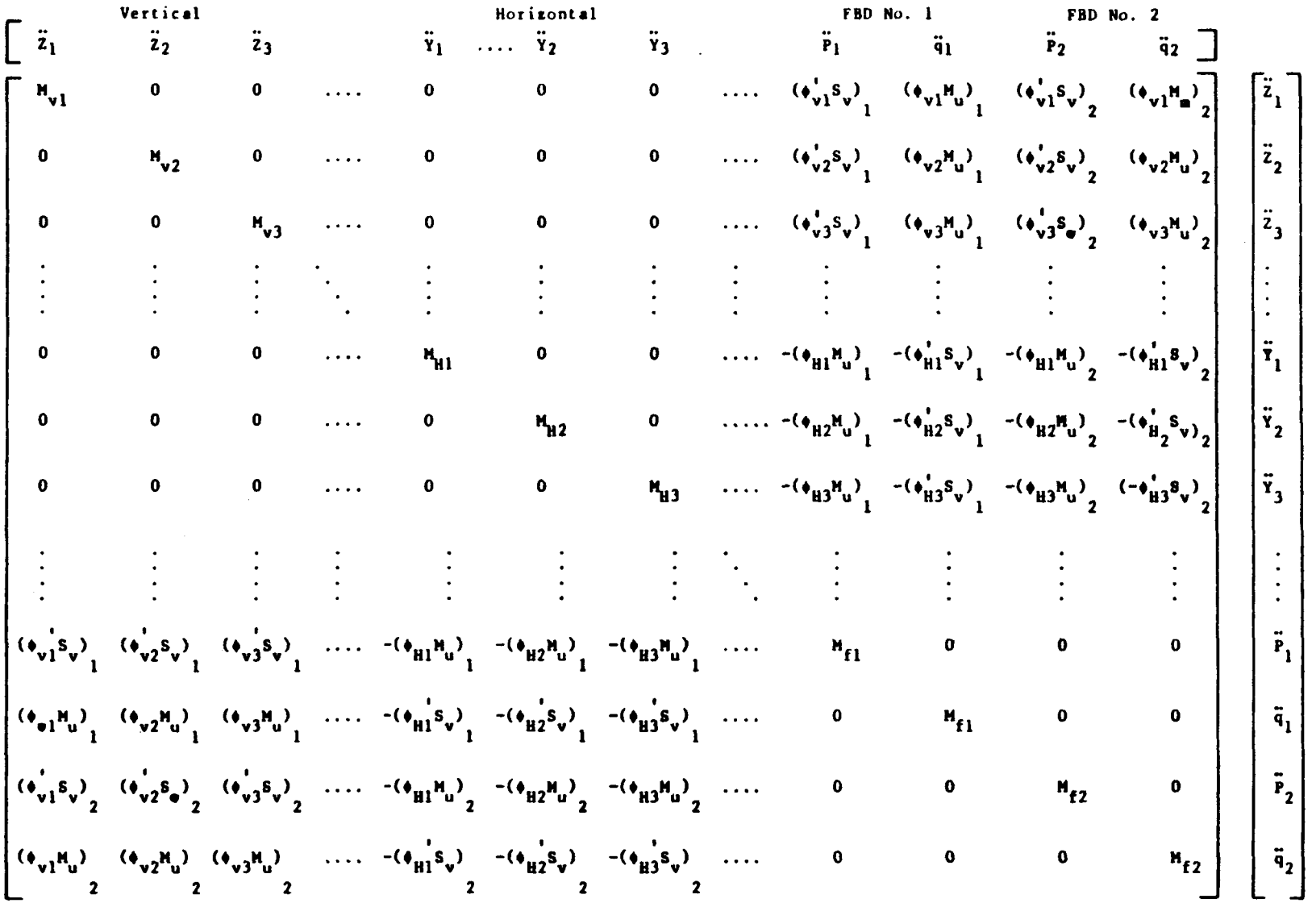

Figure 4-3. Sample Global Mass Matrix [M]

4.4.3 Global Stiffness Matrix [K]

$$[K] = [K]_{modal\ stiffness} + \sum_{i=1}^{n} [\Phi_i]^T [K_i][\Phi_i]$$

The global stiffness matrix consists of the modal stiffness terms (along the diagonal) plus the contributions of the linear (type 1, 2, 4, or 5) physical connecting elements. The contributions of each linear physical connecting element (see section 4.2.2) are added into the correct location in the [K] matrix. The [K] matrix is stored separately in TETRA. Note, however, that the modal stiffnesses of the flexible bladed disks (if any) vary with the speed of the rotor on which the flexible bladed disks are located (these are the only stiffness terms that vary with rotor speed or forcing frequency), and hence the FBD modal stiffness terms are not incorporated into the [K] matrix of TETRA but rather written directly into the global solution matrix in subroutine GLOB2.

4.4.4 Global Velocity Matrix [C]

$$[C] = [C_0] + \frac{1}{|\Omega_s|}[C_s] + \Omega_I [G_I] + \Omega_D [G_D] + \Omega_{FBD} [G_{FBD}]$$

where

$$[C_o] = [C]_{modal\ damping} + \sum_{i}^{n} [\Phi_i]^T [C_i][\Phi_i]$$

= the contributions of the modal damping plus the non-structural damping contributions of the linear (type 1, 2, 4, or 5) physical connecting elements. The contributions of each linear physical connecting element (see section 4.2.3.1) are added into the correct locations in the $[C_0]$ matrix. The $[C_0]$ matrix is the same size as the global velocity matrix [C] (square matrix whose order = total number of modes)

Ω_s = Frequency used for the structural damping. This corresponds to the independent rotor speed (if ISF = 1 on type A input sheet) or to the steady state forcing frequency (if ISF = 2 on the type A input sheet).

$$[C_s] = \sum_{i=1}^{n} \frac{1}{QF_i} [\Phi_i]^T [K_i][\Phi_i]$$

= Matrix for the structural damping contributions (not including the $1/\Omega_s$ multiplier) of the linear (type 1, 2, 4, and 5) physical connecting elements. The structural damping contributions of each linear physical connecting element (see section 4.2.3.2) are added into the correct positions in the $[C_S]$ matrix. The $[C_S]$ matrix

is the same size as the [C] matrix except that the rows and columns for the flexible bladed disks are omitted (C_S is a square matrix whose order equals the total number of modes in subsystems 1 through 11).

Ω_I = Independent rotor speed

$$[G_I] = \sum_{i=1}^{n} [\Phi_i]^T [G_i][\Phi_i]$$

= matrix for the contributions (not including the Ω_I multiplier) of the gyroscopic load points on the independent rotor. The contributions for each gyroscopic load point i (see section 4.3.2) are added into the correct positions in the $[G_I]$ matrix. The $[G_I]$ matrix is a square whose order = total number of modes for the independent rotor.

Ω_D = Dependent rotor speed

$$[G_D] = \sum_{i=1}^{n} [\Phi_I]^T [G_i][\Phi_i]$$

= matrix for the contributions (not including the Ω_D multiplier) of the gyroscopic load points on the dependent rotor. The contributions for each gyroscopic load point i (see section 4.3.2) are added into the correct position in the $[G_D]$ matrix. The $[G_D]$ matrix is a square matrix whose order = total number of modes for the dependent rotor.

Ω_{FBD} = speed of the rotor on which the flexible bladed disks are located.

$[G_{FBD}]$ = matrix for the contributions (not including the Ω_{FBD} multiplier) of the gyroscopic loading due to the flexible bladed disks. This does not include the terms for the flexible bladed disk center of gravity points, which are included in either the $[G_I]$ or the $[G_D]$ matrix. See figure 4-4 for the contents of the $[G_{FBD}]$ matrix.

The global velocity matrix [C] is not stored separately in TETRA, but the component matrices $[C_0]$, $[C_S]$, $[G_I]$, and $[G_D]$ are stored separately. The component matrix $[G_{FBD}]$ is not stored, but the non-zero terms of this matrix are stored in arrays and scalar variables. The terms of the component matrices are multiplied by the appropriate multipliers and incorporated directly into the correct positions in the global solution matrix in subroutine GLOB2.

$$
\left[G_{FBD}\right] = \left[\dot{z}_1 \quad \dot{z}_2 \quad \dot{z}_3 \quad \cdots \quad \dot{y}_1 \quad \dot{y}_2 \quad \dot{y}_3 \quad \cdots \quad \dot{p}_1 \quad \dot{q}_1 \quad \dot{p}_2 \quad \dot{q}_2\right]
$$

$$
\begin{bmatrix}
0 & 0 & 0 & \cdots & 0 & 0 & 0 & \cdots & 0 & -2\left(S_v\Phi'_{v1}\right)_1 & 0 & -2\left(S_v\Phi'_{v1}\right)_2 \\
0 & 0 & 0 & \cdots & 0 & 0 & 0 & \cdots & 0 & -2\left(S_v\Phi'_{v2}\right)_1 & 0 & -2\left(S_v\Phi'_{v2}\right)_2 \\
0 & 0 & 0 & \cdots & 0 & 0 & 0 & \cdots & 0 & -2\left(S_v\Phi'_{v3}\right)_1 & 0 & -2\left(S_v\Phi'_{v3}\right)_2 \\
\vdots & \vdots & \vdots & & \vdots & \vdots & \vdots & & \vdots & \vdots & \vdots & \vdots \\
0 & 0 & 0 & \cdots & 0 & 0 & 0 & \cdots & -2\left(S_v\Phi'_{H1}\right)_1 & 0 & -2\left(S_v\Phi'_{H1}\right)_2 & 0 \\
0 & 0 & 0 & \cdots & 0 & 0 & 0 & \cdots & -2\left(S_v\Phi'_{H2}\right)_1 & 0 & -2\left(S_v\Phi'_{H2}\right)_2 & 0 \\
0 & 0 & 0 & \cdots & 0 & 0 & 0 & \cdots & -2\left(S_v\Phi'_{H3}\right)_1 & 0 & -2\left(S_v\Phi'_{H3}\right)_2 & 0 \\
\vdots & \vdots & \vdots & & \vdots & \vdots & \vdots & & \vdots & \vdots & \vdots & \vdots \\
0 & 0 & 0 & \cdots & 2\left(S_v\Phi'_{H1}\right)_1 & 2\left(S_v\Phi'_{H2}\right)_1 & 2\left(S_v\Phi'_{H3}\right)_1 & \cdots & 0 & -2m_{f1} & 0 & 0 \\
2\left(S_v\Phi'_{v1}\right)_1 & 2\left(S_v\Phi'_{v2}\right)_1 & 2\left(S_v\Phi'_{v3}\right)_1 & \cdots & 0 & 0 & 0 & \cdots & 2m_{f1} & 0 & 0 & 0 \\
0 & 0 & 0 & \cdots & 2\left(S_v\Phi'_{H1}\right)_2 & 2\left(S_v\Phi'_{H2}\right)_2 & 2\left(S_v\Phi'_{H3}\right)_2 & \cdots & 0 & 0 & 0 & -2m_{f2} \\
2\left(S_v\Phi'_{v1}\right)_2 & 2\left(S_v\Phi'_{v2}\right)_2 & 2\left(S_v\Phi'_{v3}\right)_2 & \cdots & 0 & 0 & 0 & \cdots & 0 & 0 & 2m_{f2} & 0
\end{bmatrix}
\begin{bmatrix}
\dot{z}_1 \\ \dot{z}_2 \\ \dot{z}_3 \\ \vdots \\ \dot{y}_1 \\ \dot{y}_2 \\ \dot{y}_3 \\ \vdots \\ \dot{p}_1 \\ \dot{q}_1 \\ \dot{p}_2 \\ \dot{q}_2
\end{bmatrix}
$$

FIGURE 4-4. MATRIX $\left[G_{FBD}\right]$

4.4.5 Global Solution Matrix [GM]

Using tensor notation, our equation of motion is:

$$M_{ij}\ddot{q}_j + K_{ij}q_j + C_{ij}\dot{q}_j = F_i + H_i$$

where:

M_{ij} = global mass matrix
K_{ij} = global stiffness matrix
C_{ij} = global velocity matrix
q_j = generalized displacements
F_i = generalized applied (external) force vector
H_i = generalized nonlinear rub element force vector

We can substitute:

$$q_i = a_j \cos\omega t + b_j \sin\omega t$$
$$F_i = F_i^c \cos\omega t + F_i^s \sin\omega t$$
$$H_i = H_i^c \cos\omega t + H_i^s \sin\omega t$$

(the H_i expression is possible because we use harmonic averaging to get the nonlinear (rub) element forces, as will be shown later).

This gives:

$$-\omega^2 M_{ij}\left(a_j \cos\omega t + b_j \sin\omega t\right) + K_{ij}\left(a_j \cos\omega t + b_j \sin\omega t\right) + \omega C_{ij}\left(-a_j \sin\omega t + b_j \cos\omega t\right)$$

$$= F_i^c \cos\omega t + F_i^s \sin\omega t + H_i^c \cos\omega t + H_i^s \sin\omega t$$

Now separating out the sin and cos parts this yields two equations:

$$-\omega^2 M_{ij} a_j \cos\omega t + K_{ij} a_j \cos\omega t + \omega C_{ij} b_j \cos\omega t = F_i^c \cos\omega t + H_i^c \cos\omega t$$

$$-\omega^2 M_{ij} b_j \sin\omega t + K_{ij} b_j \sin\omega t - \omega C_{ij} a_j \sin\omega t = F_i^s \sin\omega t + H_i^s \sin\omega t$$

Dividing through *by* $\cos\omega t$ *and* $\sin\omega t$ and rewriting:

$$\left(-\omega^2 M_{ij} + K_{ij}\right)a_j + \omega C_{ij} b_j = F_i^c + H_i^c$$

$$\left(-\omega^2 M_{ij} + K_{ij}\right)b_i - \omega C_{ij} a_j = F_i^s + H_i^s$$

We can write this in matrix form as follows (also noting that $M_{ij} = 0$ for $i \neq j$):

$$\begin{bmatrix} -\omega^2 M_{11} + K_{11} & \cdots & K_{1n} & \omega C_{11} & \cdots & \omega C_{1n} \\ \vdots & \ddots & & \vdots & \ddots & \\ K_{n1} & \cdots & -\omega^2 M_{nn} + K_{nn} & \omega C_{n1} & \cdots & \omega C_{nn} \\ -\omega C_{11} & \cdots & -\omega C_{1n} & -\omega^2 M_{11} + K_{11} & \cdots & K_{1n} \\ \vdots & \ddots & & \vdots & \ddots & \\ -\omega C_{n1} & \cdots & -\omega C_{nn} & K_{n1} & \cdots & -\omega^2 M_{nn} + K_{nn} \end{bmatrix} \begin{bmatrix} a_1 \\ \\ \\ a_n \\ b_1 \\ \\ \\ b_n \end{bmatrix} = \begin{bmatrix} F_1^c \\ \\ \\ F_n^c \\ F_1^s \\ \\ \\ F_n^s \end{bmatrix} + \begin{bmatrix} H_1^c \\ \\ \\ H_n^c \\ H_1^s \\ \\ \\ H_n^s \end{bmatrix}$$

where n = number of generalized coordinates (modes)

We define the large 2n x 2n matrix on the left hand side to be the global solution matrix [GM]:

$$[GM] = \begin{bmatrix} -\omega^2 M_{11} + K_{11} & \cdots & K_{1n} & \omega C_{11} & \cdots & \omega C_{1n} \\ \vdots & \ddots & & \vdots & \ddots & \\ K_{n1} & \cdots & -\omega^2 M_{nn} + K_{nn} & \omega C_{n1} & \cdots & \omega C_{nn} \\ -\omega C_{11} & \cdots & -\omega C_{1n} & -\omega^2 M_{11} + K_{11} & \cdots & K_{1n} \\ \vdots & \ddots & & \vdots & \ddots & \\ -\omega C_{n1} & \cdots & -\omega C_{nn} & K_{n1} & \cdots & -\omega^2 M_{nn} + K_{nn} \end{bmatrix}$$

We see that knowing the elements of the global mass matrix M_{ij}, the elements of the global stiffness matrix K_{ij}, the elements of the global velocity matrix C_{ij}, and the steady state forcing frequency ω, we can calculate the global solution matrix.

Then we have:

$$\begin{bmatrix} \\ GM \\ \\ \end{bmatrix} \begin{bmatrix} a_1 \\ \vdots \\ a_n \\ b_1 \\ \vdots \\ b_n \end{bmatrix} = \begin{bmatrix} F_1^c \\ \vdots \\ F_n^c \\ F_1^s \\ \vdots \\ F_n^s \end{bmatrix} + \begin{bmatrix} H_1^c \\ \vdots \\ H_n^c \\ H_1^s \\ \vdots \\ H_n^s \end{bmatrix}$$

4.5 Iteration Method and Equations

4.5.1 General Method

We demonstrated in the previous section that the equation of motion can be written in matrix form as:

$$\begin{bmatrix} \\ GM \\ \\ \end{bmatrix} \begin{bmatrix} a_1 \\ \vdots \\ a_n \\ b_1 \\ \vdots \\ b_n \end{bmatrix} = \begin{bmatrix} F_1^c \\ \vdots \\ F_n^c \\ F_1^s \\ \vdots \\ F_n^s \end{bmatrix} + \begin{bmatrix} H_1^c \\ \vdots \\ H_n^c \\ H_1^s \\ \vdots \\ H_n^s \end{bmatrix}$$

Solving for the cosine and sine components of the generalized displacements (a_i and b_i respectively):

$$\begin{bmatrix} a_1 \\ \vdots \\ a_n \\ b_1 \\ \vdots \\ b_n \end{bmatrix} = \begin{bmatrix} \\ GM \\ \\ \end{bmatrix}^{-1} \begin{bmatrix} F_1^c \\ \vdots \\ F_n^c \\ F_1^s \\ \vdots \\ F_n^s \end{bmatrix} + \begin{bmatrix} \\ GM \\ \\ \end{bmatrix}^{-1} \begin{bmatrix} H_1^c \\ \vdots \\ H_n^c \\ H_1^s \\ \vdots \\ H_n^s \end{bmatrix}$$

We define:

$$\begin{bmatrix} R_1^c \\ \vdots \\ R_n^c \\ R_1^s \\ \vdots \\ R_n^s \end{bmatrix} = \begin{bmatrix} \quad \\ GM \\ \quad \end{bmatrix}^{-1} \begin{bmatrix} F_1^c \\ \vdots \\ F_n^c \\ F_1^s \\ \vdots \\ F_n^s \end{bmatrix} = R \text{ Vector}$$

and

$$\begin{bmatrix} T_1^c \\ \vdots \\ T_n^c \\ T_1^s \\ \vdots \\ T_n^s \end{bmatrix} = \begin{bmatrix} \quad \\ GM \\ \quad \end{bmatrix}^{-1} \begin{bmatrix} H_1^c \\ \vdots \\ H_n^c \\ H_1^s \\ \vdots \\ H_n^s \end{bmatrix} = T \text{ Vector}$$

Then we have:

$$\begin{bmatrix} a_1 \\ \vdots \\ a_n \\ b_1 \\ \vdots \\ b_n \end{bmatrix} = \begin{bmatrix} R_1^c \\ \vdots \\ R_n^c \\ R_1^s \\ \vdots \\ R_n^s \end{bmatrix} + \begin{bmatrix} T_1^c \\ \vdots \\ T_n^c \\ T_1^s \\ \vdots \\ T_n^s \end{bmatrix}$$

Expanding the T vector in the above we get:

$$\begin{bmatrix} a_1 \\ \vdots \\ a_n \\ b_1 \\ \vdots \\ b_n \end{bmatrix} = \begin{bmatrix} R_1^c \\ \vdots \\ R_n^c \\ R_1^s \\ \vdots \\ R_n^s \end{bmatrix} + \begin{bmatrix} g_{1,1}H_1^c + \ldots + g_{1,n}H_n^c + g_{1,n+1}H_1^s + \ldots g_{1,2n}H_n^s \\ \vdots \\ g_{n,1}H_1^c + \ldots + g_{n,n}H_n^c + g_{n,n+1}H_1^s + \ldots g_{n,2n}H_n^s \\ g_{n+1,1}H_1^c + \ldots + g_{n+1,n}H_n^c + g_{n+1,n+1}H_1^s + \ldots g_{n+1,2n}H_n^s \\ \vdots \\ g_{2n,1}H_1^c + \ldots + g_{2n,n}H_n^c + g_{2n,n+1}H_1^s + \ldots g_{2n,2n}H_n^s \end{bmatrix} \quad (1)$$

where the $g_{i,j}$ are the elements of the inverse of the global solution matrix $[GM]^{-1}$.

The g_{ij} values (elements of the inverse of the global solution matrix) are found in a straight forward manner by first finding the global solution matrix [GM] as detailed previously, then inverting the global solution matrix. The R_i^c and R_i^s values (the R vector) can also be calculated in a straight forward manner by multiplying the inverse of the global solution matrix by the applied (external) force vector F (also easily found), as per the definition of the R vector.

If there are no nonlinear (rub) elements, or if there is no rub because the dead band has not been exceeded for any rub element, then the sine and cosine components of the generalized nonlinear (rub) element forces (the H_i^c and H_i^s respectively) are zero. For this case, the cosine and sine components of the generalized displacements (the a_i and b_i respectively) can be found easily since they are equal to the R_i^c and R_i^s values, and we're done. However, if nonlinear (rub) elements are present, and if there is a rub for at least one of the rub elements, then we must find the H_i^c and H_i^s values, which becomes much more involved.

To find the H_i^c and H_i^s values (if needed) iteration must be performed. This is done by deriving a set of iterating equations in which the rub element relative displacement components (the Δx's) are the unknowns. For each iteration, we calculate the rub element physical force components at joint I (the P's), which are functions of the Δx's , and which get plugged into the iterating equations. Then, after the iterating equations have (hopefully) converged to a solution, we take the final values for the rub element physical force components at joint I (the P's), and calculate the nonlinear (rub) element generalized force components (the H_i^c and H_i^s values) (the H vector).

The rest is simple. The T vector is then found by multiplying the inverse of the global solution matrix by the H vector as per the definition of the T vector. The R vector and the T vectors are then added together to find the cosine and sine components of the generalized displacements (the a_i and b_i respectively).

The following sections detail the derivation of the iterating equations and the derivation of the rub element physical forces at joint I.

4.5.2 Derivation of the Iterating Equations

We can write:

$$\Delta X_{k,v} = \Delta X^c_{k,v} \cos \omega t + \Delta X^s_{k,v} \sin \omega t$$

$$\Delta X_{k,H} = \Delta X^c_{k,H} \cos \omega t + \Delta X^s_{k,H} \sin \omega t$$

where $\Delta X_{k,v}$ = relative displacement for the k'th nonlinear (rub) element in the vertical direction

$\Delta X_{k,H}$ = relative displacement for the k'th nonlinear (rub) element in the horizontal direction

For each nonlinear (rub) element k, we have four equation as follows:

$$\Delta X^c_{k,v} = X^c_{k,v,I} - X^c_{k,v,J} = \sum_{i=1}^{n} a_i \left(\Phi_{k,i,v,I} - \Phi_{k,i,v,J} \right) \quad (2)$$

$$\Delta X^c_{k,H} = X^c_{k,H,I} - X^c_{k,H,J} = \sum_{i=1}^{n} a_i \left(\Phi_{k,i,H,I} - \Phi_{k,i,H,J} \right) \quad (3)$$

$$\Delta X^s_{k,v} = X^s_{k,v,I} - X^s_{k,v,J} = \sum_{i=1}^{n} b_i \left(\Phi_{k,i,v,I} - \Phi_{k,i,v,J} \right) \quad (4)$$

$$\Delta X^s_{k,H} = X^s_{k,H,I} - X^s_{k,H,J} = \sum_{i=1}^{n} b_i \left(\Phi_{k,i,H,I} - \Phi_{k,i,H,J} \right) \quad (5)$$

where $X^{c\ or\ s}_{k,v\ or\ H,I\ or\ J}$ = cosine(c) or sin (s) component of the vertical (V) or horizontal (H) displacement for joint I (I) or joint J (J) for the k'th nonlinear rub element

$\Phi_{k,i,v\ or\ H,I\ or\ J}$ = Mode shape for k'th nonlinear (rub) element, mode i, vertical (V) or horizontal (H), joint I (I) or joint J (J)

a_i = cos component of the generalized displacement for mode i

b_i = sin component of the generalized displacement for mode i

We now define:

$$\Delta\Phi_{k,i,v} = \Phi_{k,i,v,I} - \Phi_{k,i,v,J}$$

$$\Delta\Phi_{k,i,H} = \Phi_{k,i,H,I} - \Phi_{k,i,H,J}$$

Substituting this into equations 2 through 5 we have:

$$\Delta X^{c}_{k,v} = \sum_{i=1}^{n} a_i \Delta\Phi_{k,i,v}$$

$$\Delta X^{c}_{k,H} = \sum_{i=1}^{n} a_i \Delta\Phi_{k,i,H}$$

$$\Delta X^{s}_{k,v} = \sum_{i=1}^{n} b_i \Delta\Phi_{k,i,v}$$

$$\Delta X^{s}_{k,H} = \sum_{i=1}^{n} b_i \Delta\Phi_{k,i,H}$$

Further, we can define

$$F^{c}_{k,v} = \sum_{i=1}^{n} a_i \Delta\Phi_{k,i,v} - \Delta X^{c}_{k,v} = 0 \qquad (6)$$

$$F^{c}_{k,H} = \sum_{i=1}^{n} a_i \Delta\Phi_{k,i,H} - \Delta X^{c}_{k,H} = 0 \qquad (7)$$

$$F^{s}_{k,v} = \sum_{i=1}^{n} b_i \Delta\Phi_{k,i,v} - \Delta X^{s}_{k,v} = 0 \qquad (8)$$

$$F^{s}_{k,H} = \sum_{i=1}^{n} b_i \Delta\Phi_{k,i,H} - \Delta X^{s}_{k,H} = 0 \qquad (9)$$

where $F^{c\ or\ s}_{k,v\ or\ H}$ = the iterating equation for the k'th rub element, cosine (c) or sin (s) component in the vertical (V) or horizontal (H) direction

The unknowns in the iterating equations are the relative displacement components $\left(\Delta X^{c}_{k,v},\ \Delta X^{c}_{k,H},\ \Delta X^{s}_{k,v},\ \Delta X^{s}_{k,H}\right)$. During iteration the values of the $\left(F^{c}_{k,v},\ F^{c}_{k,H},\ F^{s}_{k,v},\ F^{s}_{k,H}\right)$ expressions approach 0 as the unknowns approach their true value. The number of iterating equations equals 4 times the number of nonlinear (rub) elements.

From equation 1 we see that:

$$a_i = R_i^c + \sum_{j=1}^{n} g_{i,j} H_j^c + \sum_{j=1}^{n} g_{i,n+j} H_j^s$$

$$b_i = R_i^s + \sum_{j=1}^{n} g_{n+i,j} H_j^c + \sum_{j=1}^{n} g_{n+i,n+j} H_j^s$$

Plugging the a_i and b_i expressions into the iterating equations (equations 6 through 9) we get:

$$F_{k,v}^c = \sum_{i=1}^{n} \left(R_i^c + \sum_{j=1}^{n} g_{i,j} H_j^c + \sum_{j=1}^{n} g_{i,n+j} H_j^s \right) \Delta\Phi_{k,i,v} - \Delta X_{k,v}^c = 0$$

$$F_{k,H}^c = \sum_{i=1}^{n} \left(R_i^c + \sum_{j=1}^{n} g_{i,j} H_j^c + \sum_{j=1}^{n} g_{i,n+j} H_j^s \right) \Delta\Phi_{k,i,H} - \Delta X_{k,H}^c = 0$$

$$F_{k,v}^s = \sum_{i=1}^{n} \left(R_i^s + \sum_{j=1}^{n} g_{n+i,j} H_j^c + \sum_{j=1}^{n} g_{n+1,n+j} H_j^s \right) \Delta\Phi_{k,i,v} - \Delta X_{k,v}^s = o$$

$$F_{k,H}^s = \sum_{i=1}^{n} \left(R_i^s + \sum_{j=1}^{n} g_{n+i,j} H_j^c + \sum_{j=1}^{n} g_{n+i,n+j} H_j^s \right) \Delta\Phi_{k,i,H} - \Delta X_{k,H}^s = 0$$

Now defining:

$$\sum_{i=1}^{n} R_i^c \ \Delta\Phi_{k,i,v} = S_{k,v}^c$$

$$\sum_{i=1}^{n} R_i^c \ \Delta\Phi_{k,i,H} = S_{k,H}^c$$

$$\sum_{i=1}^{n} R_i^s \ \Delta\Phi_{k,i,v} = S_{k,v}^s$$

$$\sum_{i=1}^{n} R_i^s \ \Delta\Phi_{k,i,H} = S_{k,H}^s$$

We can write:

$$F_{k,v}^c = S_{k,v}^c + \sum_{i=1}^{n} \Delta\Phi_{k,i,v} \sum_{j=1}^{n} g_{i,j} H_j^c + \sum_{i=1}^{n} \Delta\Phi_{k,i,v} \sum_{j=1}^{n} g_{i,n+j} H_j^s - \Delta X_{k,v}^c = 0 \qquad (10)$$

$$F_{k,H}^c = S_{k,H}^c + \sum_{i=1}^{n} \Delta\Phi_{k,i,H} \sum_{j=1}^{n} g_{i,j} H_j^c + \sum_{i=1}^{n} \Delta\Phi_{k,i,H} \sum_{j=1}^{n} g_{i,n+j} H_j^s - \Delta X_{k,H}^c = 0 \qquad (11)$$

$$F_{k,v}^s = S_{k,v}^s + \sum_{i=1}^{n} \Delta\Phi_{k,i,v} \sum_{j=1}^{n} g_{n+i,j} H_j^c + \sum_{i=1}^{n} \Delta\Phi_{k,i,v} \sum_{j=1}^{n} g_{n+i,n+j} H_j^s - \Delta X_{k,v}^s = 0 \qquad (12)$$

$$F_{k,H}^s = S_{k,H}^s + \sum_{i=1}^{n} \Delta\Phi_{k,i,H} \sum_{j=1}^{n} g_{n+i,j} H_j^c + \sum_{i=1}^{n} \Delta\Phi_{k,i,H} \sum_{j=1}^{n} g_{n+i,n+j} H_j^s - \Delta X_{k,H}^s = 0 \qquad (13)$$

To get the generalized nonlinear force (the H's) we add the contributions of joint I (subscript I) and joint J (subscript J) in both the vertical (subscript V) and horizontal (subscript H) directions and sum over the nonlinear elements:

$$H^c_j = \sum_{\ell=1}^{L} \left(H^c_{j,v,I} + H^c_{j,H,I} + H^c_{j,v,J} + H^c_{j,H,J} \right)$$

$$H^s_j = \sum_{\ell=1}^{L} \left(H^s_{j,v,I} + H^s_{j,H,I} + H^s_{j,v,J} + H^s_{j,H,J} \right)$$

To get each H contribution we multiply the mode shape Φ by the nonlinear connecting element force P.

$$H^c_j = \sum_{\ell=1}^{L} \left(\Phi_{\ell,j,v,I} \; P^c_{\ell,v,I} + \Phi_{\ell,j,H,I} \; P^c_{\ell,H,I} + \Phi_{\ell,j,v,J} \; P^c_{\ell,v,J} + \Phi_{\ell,j,H,J} \; P^c_{\ell,H,J} \right)$$

$$H^s_j = \sum_{\ell=1}^{L} \left(\Phi_{\ell,j,v,I} \; P^s_{\ell,v,I} + \Phi_{\ell,j,H,I} \; P^s_{\ell,H,I} + \Phi_{\ell,j,v,J} \; P^s_{\ell,v,J} + \Phi_{\ell,j,H,J} \; P^s_{\ell,H,J} \right)$$

Noting that:

$$P^c_{\ell,v,J} = -P^c_{\ell,v,I} \; ; \; P^c_{\ell,H,J} = -P^c_{\ell,H,I}$$

$$P^s_{\ell,v,J} = -P^s_{\ell,v,I} \; ; \; P^s_{\ell,H,J} = -P^s_{\ell,H,I}$$

we get:

$$H^c_j = \sum_{\ell=1}^{L} \left[P^c_{\ell,v,I} \left(\Phi_{\ell,j,v,I} - \Phi_{\ell,j,v,J} \right) + P^c_{\ell,H,I} \left(\Phi_{\ell,j,H,I} - \Phi_{\ell,j,H,J} \right) \right]$$

$$H^s_j = \sum_{\ell=1}^{L} \left[P^s_{\ell,v,I} \left(\Phi_{\ell,j,v,I} - \Phi_{\ell,j,v,J} \right) + P^s_{\ell,H,I} \left(\Phi_{\ell,j,H,I} - \Phi_{\ell,j,H,J} \right) \right]$$

Defining:

$$\Delta\Phi_{\ell,j,v} = \Phi_{\ell,j,v,I} - \Phi_{\ell,j,v,J}$$

$$\Delta\Phi_{\ell,j,H} = \Phi_{\ell,j,H,I} - \Phi_{\ell,j,H,J}$$

we get:

$$H_j^c = \sum_{\ell=1}^{L} \left(P^c_{\ell,v,I}\,\Delta\Phi_{\ell,j,v} + P^c_{\ell,H,I}\,\Delta\Phi_{\ell,j,H} \right) \tag{14}$$

$$H_j^s = \sum_{\ell=1}^{L} \left(P^s_{\ell,v,I}\,\Delta\Phi_{\ell,j,v} + P^s_{\ell,H,I}\,\Delta\Phi_{\ell,j,H} \right) \tag{15}$$

Substituting these expressions for H_j^c and H_j^s into equations 10 through 13 we get:

$$F^c_{k,v} = S^c_{k,v} + \sum_{i=1}^{n} \Delta\phi_{k,i,v} \sum_{j=1}^{n} g_{i,j} \sum_{\ell=1}^{L} \left(P^c_{\ell,v,I}\,\Delta\phi_{\ell,j,v} + P^c_{\ell,H,I}\,\Delta\phi_{\ell,j,H} \right) + \sum_{i=1}^{n} \Delta\phi_{k,i,v} \sum_{j=1}^{n} g_{i,n+j} \sum_{\ell=1}^{L} \left(P^s_{\ell,v,I}\,\Delta\phi_{\ell,j,v} + P^s_{\ell,H,I}\,\Delta\phi_{\ell,j,H} \right) - \Delta X^c_{k,v} = 0$$

$$F^c_{k,H} = S^c_{k,H} + \sum_{i=1}^{n} \Delta\phi_{k,i,H} \sum_{j=1}^{n} g_{i,j} \sum_{\ell=1}^{L} \left(P^c_{\ell,v,I}\,\Delta\phi_{\ell,j,v} + P^c_{\ell,H,I}\,\Delta\phi_{\ell,j,H} \right) + \sum_{i=1}^{n} \Delta\phi_{k,i,H} \sum_{j=1}^{n} g_{i,n+j} \sum_{\ell=1}^{L} \left(P^s_{\ell,v,I}\,\Delta\phi_{\ell,j,v} + P^s_{\ell,H,I}\,\Delta\phi_{\ell,j,H} \right) - \Delta X^c_{k,H} = 0$$

$$F^s_{k,v} = S^s_{k,v} + \sum_{i=1}^{n} \Delta\Phi_{k,i,v} \sum_{j=1}^{n} g_{n+i,j} \sum_{\ell=1}^{L} \left(P^c_{\ell,v,I}\,\Delta\Phi_{\ell,j,v} + P^c_{\ell,H,I}\,\Delta\Phi_{\ell,j,H} \right) + \sum_{i=1}^{n} \Delta\Phi_{k,i,v} \sum_{j=1}^{n} g_{n+i,n+j} \sum_{\ell=1}^{L} \left(P^s_{\ell,v,I}\,\Delta\Phi_{\ell,j,v} + P^s_{\ell,H,I}\,\Delta\Phi_{\ell,j,H} \right) - \Delta X^s_{k,s} = 0$$

$$F^s_{k,H} = S^s_{k,H} + \sum_{i=1}^{n} \Delta\phi_{k,i,H} \sum_{j=1}^{n} g_{n+i,j} \sum_{\ell=1}^{L} \left(P^c_{\ell,v,I}\,\Delta\phi_{\ell,j,v} + P^c_{\ell,H,I}\,\Delta\phi_{\ell,j,H} \right) + \sum_{i=1}^{n} \Delta\phi_{k,i,H} \sum_{j=1}^{n} g_{n+i,n+j} \sum_{\ell=1}^{L} \left(P^s_{\ell,v,I}\,\Delta\phi_{\ell,j,v} + P^s_{\ell,H,I}\,\Delta\phi_{\ell,j,H} \right) - \Delta X^s_{k,H} = 0$$

Rewriting:

$$F^c_{k,v} = S^c_{k,v} + \sum_{i=1}^{n} \Delta\phi_{k,i,v} \sum_{j=1}^{n} g_{i,j} \sum_{\ell=1}^{L} \Delta\phi_{\ell,j,v}\ P^c_{\ell,v,I} + \sum_{i=1}^{n} \Delta\phi_{k,i,v} \sum_{j=1}^{n} g_{i,j} \sum_{\ell=1}^{L} \Delta\phi_{\ell,j,H}\ P^c_{\ell,H,I} \tag{16}$$

$$+ \sum_{i=1}^{n} \Delta\phi_{k,i,v} \sum_{j=1}^{n} g_{i,n+j} \sum_{\ell=1}^{L} \Delta\phi_{\ell,j,v}\ P^s_{\ell,v,I} + \sum_{i=1}^{n} \Delta\phi_{k,i,v} \sum_{j=1}^{n} g_{i,n+j} \sum_{\ell=1}^{L} \Delta\phi_{\ell,j,H}\ P^s_{\ell,H,I}$$

$$-\Delta X^c_{k,v} = 0$$

$$F^c_{k,H} = S^c_{k,H} + \sum_{i=1}^{n} \Delta\phi_{k,i,H} \sum_{j=1}^{n} g_{i,j} \sum_{\ell=1}^{L} \Delta\phi_{\ell,j,v}\ P^c_{\ell,v,I} + \sum_{i=1}^{n} \Delta\phi_{k,i,H} \sum_{j=1}^{n} g_{i,j} \sum_{\ell=1}^{L} \Delta\phi_{\ell,j,H}\ P^c_{\ell,H,I} \tag{17}$$

$$+ \sum_{i=1}^{n} \Delta\phi_{k,i,H} \sum_{j=1}^{n} g_{i,n+j} \sum_{\ell=1}^{L} \Delta\phi_{\ell,j,v}\ P^s_{\ell,v,I} + \sum_{i=1}^{n} \Delta\phi_{k,i,H} \sum_{j=1}^{n} g_{i,n+j} \sum_{\ell=1}^{L} \Delta\phi_{\ell,j,H}\ P^s_{\ell,H,I}$$

$$-\Delta X^c_{k,H} = 0$$

$$F^s_{k,v} = S^s_{k,v} + \sum_{i=1}^{n} \Delta\phi_{k,i,v} \sum_{j=1}^{n} g_{n+i,j} \sum_{\ell=1}^{L} \Delta\phi_{\ell,j,v}\ P^c_{\ell,v,I} + \sum_{i=1}^{n} \Delta\phi_{k,i,v} \sum_{j=1}^{n} g_{n+i,j} \sum_{\ell=1}^{L} \Delta\phi_{\ell,j,H} P^c_{\ell,H,I} \tag{18}$$

$$+ \sum_{i=1}^{n} \Delta\phi_{k,i,v} \sum_{j=1}^{n} g_{i,n+j} \sum_{\ell=1}^{L} \Delta\phi_{\ell,j,v}\ P^s_{\ell,v,I} + \sum_{i=1}^{n} \Delta\phi_{k,i,v} \sum_{j=1}^{n} g_{n+i,n+j} \sum_{\ell=1}^{L} \Delta\phi_{\ell,j,H}\ P^s_{\ell,H,I}$$

$$-\Delta X^s_{k,v} = 0$$

$$F^s_{k,H} = S^s_{k,H} + \sum_{i=1}^{n} \Delta\phi_{k,i,H} \sum_{j=1}^{n} g_{n+i,j} \sum_{\ell=1}^{L} \Delta\phi_{\ell,j,v} P^c_{\ell,v,I} + \sum_{i=1}^{n} \Delta\phi_{k,i,H} \sum_{j=1}^{n} g_{n+i,j} \sum_{\ell=1}^{L} \Delta\phi_{\ell,j,H} P^c_{\ell,H,I} \tag{19}$$

$$+ \sum_{i=1}^{n} \Delta\phi_{k,i,H} \sum_{j=1}^{n} g_{n+i,n+j} \sum_{\ell=1}^{L} \Delta\phi_{\ell,j,v}\ P^s_{\ell,v,I} + \sum_{i=1}^{n} \Delta\phi_{k,i,H} \sum_{j=1}^{n} g_{n+i,n+j} \sum_{\ell=1}^{L} \Delta\phi_{\ell,j,H}\ P^s_{\ell,H,I}$$

$$-\Delta X^s_{k,H} = 0$$

We define the following parameters:

$$A^{c}_{k,\upsilon,\ell} = \sum_{i=1}^{n} \Delta\phi_{k,i,\upsilon} \sum_{j=1}^{n} g_{i,j}\, \Delta\phi_{\ell,j,\upsilon}$$

$$A^{c}_{k,H,\ell} = \sum_{i=1}^{n} \Delta\phi_{k,i,H} \sum_{j=1}^{n} g_{i,j}\, \Delta\phi_{\ell,j,\upsilon}$$

$$A^{s}_{k,\upsilon,\ell} = \sum_{i=1}^{n} \Delta\phi_{k,i,\upsilon} \sum_{j=1}^{n} g_{n+i,j}\, \Delta\phi_{\ell,j,\upsilon}$$

$$A^{s}_{k,H,\ell} = \sum_{i=1}^{n} \Delta\phi_{k,i,H} \sum_{j=1}^{n} g_{n+i,j}\, \Delta\phi_{\ell,j,\upsilon}$$

$$B^{c}_{k,\upsilon,\ell} = \sum_{i=1}^{n} \Delta\phi_{k,i,\upsilon} \sum_{j=1}^{n} g_{i,j}\, \Delta\phi_{\ell,j,H}$$

$$B^{c}_{k,H,\ell} = \sum_{i=1}^{n} \Delta\phi_{k,i,H} \sum_{j=1}^{n} g_{i,j}\, \Delta\phi_{\ell,j,H}$$

$$B^{s}_{k,\upsilon,\ell} = \sum_{i=1}^{n} \Delta\phi_{k,i,\upsilon} \sum_{j=1}^{n} g_{n+i,j}\, \Delta\phi_{\ell,j,H}$$

$$B^{s}_{k,H,\ell} = \sum_{i=1}^{n} \Delta\phi_{k,i,H} \sum_{j=1}^{n} g_{n+i,j}\, \Delta\phi_{\ell,j,H}$$

$$C^{c}_{k,\upsilon,\ell} = \sum_{i=1}^{n} \Delta\phi_{k,i,\upsilon} \sum_{j=1}^{n} g_{i,n+j}\, \Delta\phi_{\ell,j,\upsilon}$$

$$C^{c}_{k,H,\ell} = \sum_{i=1}^{n} \Delta\phi_{k,i,H} \sum_{j=1}^{n} g_{i,n+j}\, \Delta\phi_{\ell,j,\upsilon}$$

$$C^{s}_{k,\upsilon,\ell} = \sum_{i=1}^{n} \Delta\phi_{k,i,\upsilon} \sum_{j=1}^{n} g_{n+i,n+j}\, \Delta\phi_{\ell,j,\upsilon}$$

$$C^{s}_{k,H,\ell} = \sum_{i=1}^{n} \Delta\phi_{k,i,H} \sum_{j=1}^{n} g_{n+i,n+j}\, \Delta\phi_{\ell,j,\upsilon}$$

$$D^{c}_{k,\upsilon,\ell} = \sum_{i=1}^{n} \Delta\phi_{k,i,\upsilon} \sum_{j=1}^{n} g_{i,n+j}\, \Delta\phi_{\ell,j,H}$$

$$D^{c}_{k,H,\ell} = \sum_{i=1}^{n} \Delta\phi_{k,i,H} \sum_{j=1}^{n} g_{i,n+j}\, \Delta\phi_{\ell,j,H}$$

$$D^{s}_{k,\upsilon,\ell} = \sum_{i=1}^{n} \Delta\phi_{k,i,\upsilon} \sum_{j=1}^{n} g_{n+i,n+j}\, \Delta\phi_{\ell,j,H}$$

$$D^{s}_{k,H,\ell} = \sum_{i=1}^{n} \Delta\phi_{k,i,H} \sum_{j=1}^{n} g_{n+i,n+j}\, \Delta\phi_{\ell,j,H}$$

Substituting these parameters into equations 16 through 19 we get:

$$F^c_{k,\upsilon} = S^c_{k,\upsilon} + \sum_{\ell=1}^{L} \left(A^c_{k,\upsilon,\ell} P^c_{\ell,\upsilon,I} + B^c_{k,\upsilon,\ell} P^c_{\ell,H,I} + C^c_{k,\upsilon,\ell} P^s_{\ell,\upsilon,I} + D^c_{k,\upsilon,\ell} P^s_{\ell,H,I} \right) - \Delta X^c_{k,\upsilon} = 0 \qquad (20)$$

$$F^c_{k,H} = S^c_{k,H} + \sum_{\ell=1}^{L} \left(A^c_{k,H,\ell} P^c_{\ell,\upsilon,I} + B^c_{k,H,\ell} P^c_{\ell,H,I} + C^c_{k,H,\ell} P^s_{\ell,\upsilon,I} + D^c_{k,H,\ell} P^s_{\ell,H,I} \right) - \Delta X^c_{k,H} = 0 \qquad (21)$$

$$F^s_{k,\upsilon} = S^s_{k,\upsilon} + \sum_{\ell=1}^{L} \left(A^s_{k,\upsilon,\ell} P^c_{\ell,\upsilon,I} + B^s_{k,\upsilon,\ell} P^c_{\ell,H,I} + C^s_{k\upsilon,\ell} P^s_{\ell,\upsilon,I} + D^s_{k,\upsilon,\ell} P^s_{\ell,H,I} \right) - \Delta X^s_{k,\upsilon} = 0 \qquad (22)$$

$$F^s_{k,H} = S^s_{k,H} + \sum_{\ell=1}^{L} \left(A^s_{k,H,\ell} P^c_{\ell,\upsilon,I} + B^s_{k,H,\ell} P^c_{\ell,H,I} + C^s_{k,H,\ell} P^s_{\ell,\upsilon,I} + D^s_{k,H,\ell} P^s_{\ell,H,I} \right) - \Delta X^s_{k,H} = 0 \qquad (23)$$

These are the iterating equations. The $F^c_{k,\upsilon}$, $F^c_{k,H}$, $F^s_{k,\upsilon}$, and $F^s_{k,H}$ functions are calculated in subroutine FCN. The actual iteration is performed either by IMSL subroutine ZSCNT or IMSL subroutine ZSPOW, depending on which of these routines the user specified via the nonlinear routine option IROUT (see input sheet I-2).

The S, A, B, C, and D parameters in the iterating equations are known quantities and are calculated based on the proceeding definitions of these quantities. Because the S, A, B, C, and D parameters do not change from iteration to iteration, for efficiency purposes they are calculated only once for each forced frequency, prior to iterating for the forced frequency. The $\Delta X's$ are the unknowns in the iterating equations. The P's in the iterating equations (the rub element forces at joint I) are functions of the $\Delta X's$. See section 5 for a discussion of the method and the equations used to find the P's.

4.5.3 Equations for the Maximum and Minimum Relative Displacement Magnitudes

The maximum and minimum relative displacement magnitudes for each rub element are needed to determine (through comparison with the dead band) if there is a rub for the given rub element and, if so, whether the rub is continual or intermittent.

As noted previously:

$$\Delta X_{k,\upsilon} = \Delta X^c_{k,\upsilon} \cos \omega t + \Delta X^s_{k,\upsilon} \sin \omega t$$

$$\Delta X_{k,H} = \Delta X^c_{k,H} \cos \omega t + \Delta X^s_{k,H} \sin \omega t$$

where

$\Delta X_{k,v}$ = relative displacement for the k'th nonlinear (rub) element in the vertical direction

$\Delta X_{k,H}$ = relative displacement for the k'th nonlinear (rub) element in the horizontal direction

We next define:

$$\Delta X^m_{k,v} = \sqrt{\left(\Delta X^c_{k,v}\right)^2 + \left(\Delta X^s_{k,v}\right)^2}$$

$$\Delta X^m_{k,H} = \sqrt{\left(\Delta X^c_{k,H}\right)^2 + \left(\Delta X^s_{k,H}\right)^2}$$

$$\Phi_v = tan^{-1}\frac{\Delta X^s_{k,v}}{\Delta X^c_{k,v}}$$

$$\Phi_H = tan^{-1}\frac{\Delta X^s_{k,H}}{\Delta X^c_{k,H}}$$

$$\Phi = \Phi_v - \Phi_H$$

Let

$\left|\Delta_k\right|_{max}$ = Maximum relative displacement magnitude for the k'th nonlinear (rub) element

$\left|\Delta_k\right|_{min}$ = Minimum relative displacement magnitude for the k'th nonlinear (rub) element

It can be shown (through the derivation is long-winded, so we skip it here):

$$\left|\Delta_k\right|_{max} = \sqrt{\frac{\left(\Delta X^m_{k,v}\right)^2+\left(\Delta X^m_{k,H}\right)^2}{2} + \frac{1}{2}\sqrt{\left(\Delta X^m_{k,v}\right)^4+\left(\Delta X^m_{k,H}\right)^4+2\left(\Delta X^m_{k,v}\right)^2\left(\Delta X^m_{k,H}\right)^2 cos\,2\Phi}} \qquad (24)$$

$$\left|\Delta_k\right|_{min} = \sqrt{\frac{\left(\Delta X^m_{k,v}\right)^2+\left(\Delta X^m_{k,H}\right)^2}{2} - \frac{1}{2}\sqrt{\left(\Delta X^m_{k,v}\right)^4+\left(\Delta X^m_{k,H}\right)^4+2\left(\Delta X^m_{k,v}\right)^2\left(\Delta X^m_{k,H}\right)^2 cos\,2\Phi}} \qquad (25)$$

4.5.4 Determining If a Rub Is Present (That is, if Iteration is Needed)

Iteration is needed to find the $\Delta X's$ (rub element relative displacement components) only if there is a rub for a least one of the rub elements. The procedure used to determine if a rub is present is as follows. First, the S parameters are found (subroutine PARAM1). Then, in subroutine CHECK, we find the $\Delta X's$ that would result assuming there were no rub element forces (that is, if the P forces were all equal to 0). From equations 20 through 23, these are:

$$\Delta X^c_{k,v} = S^c_{k,v} \qquad (26)$$

$$\Delta X^c_{k,H} = S^c_{k,H} \qquad (27)$$

$$\Delta X^s_{k,v} = S^s_{k,v} \qquad (28)$$

$$\Delta X^s_{k,H} = S^s_{k,H} \qquad (29)$$

} (assuming no rub element forces)

Then, using these $\Delta X's$ (calculated assuming no rub element forces), we calculate the maximum and minimum relative displacement magnitude for each rub element that would result assuming no rub element forces from equation 24 and 25. By comparing the maximum relative displacement magnitude with the dead band for each rub element, we can check (as we do in subroutine CHECK) if a rub is present for any each rub element.

If this check reveals that there is no rub for any of the rub elements, then we know that the assumption of no rub element forces was correct. If this is the case, then the $\Delta X's$ obtained from equations 26 through 29 are in fact the correct $\Delta X's$, and no iteration is needed. On the other hand, if this check reveals that there is a rub for at least one of the rub elements, then there are rub element forces, and equations 26 through 29 do not yield the correct $\Delta X's$. For this case, the $\Delta X's$ must be found via iteration using equations 20 through 23.

4.5.5 Finding the Initial Guess for the Iteration

Assuming that we have found that iteration is needed (see section 4.5.4), then we must find the initial guess for the iteration. This is done in subroutine check. The initial guess is determined from the following rules:

1. If it is the very first solution (forced frequency), and the user inputted an initial guess via the GUESS input variable (see namelist input sheet I-3), then the initial guess inputted by the user is used.

2. If it is the very first solution (forced frequency), and the user did not input an initial guess, then the initial guess for the rub element relative displacement components are those that would result if there were

no rub element forces (obtained from equations 26 through 29).

3. If it is not the first solution, but if rotor speed is considered for the run, there are no unbalance forces, and if it is the beginning forcing frequency for the current rotor speed, then the initial guess for the rub element relative displacement components are those that would result if there were no rub element forces (obtained from equations 26 through 29).

4. If rules 1, 2, and 3 do not apply, and if the previous frequency had a rub for at least one rub element, then the rub element relative displacements (found via iteration) for the previous forcing frequency are used as the initial guess for the iteration.

5. If rules 1, 2, and 3 do not apply, and if the previous forcing frequency did not have a rub for any of the rub elements, then the initial guess for the rub element relative displacement components are those that would result if there were no rub element forces (obtained from equations 26 through 29).

4.5.6 Solving the Iterating Equations

Assuming that we found that iteration was needed (see section 4.5.4), the first step performed is to find the initial guess for the rub element relative displacement components (see section 4.5.5). Next, we proceed to find the A, B, C, and D parameters (subroutine PARAM 2) that appear in the iterating equations. Then a whole bunch of subroutines are called (if needed) to solve the iterating equations (subroutines SOLVE, NLFORP, BACKS, FCN, plus IMSL subroutine ZSCNT or ZSPOW and several other IMSL subroutines or function subprograms which are called by ZSCNT or ZSPOW). If there is no rub for any rub element (so that iteration is not needed), all of these subroutines are skipped.

The user specifies which of two IMSL subroutines (ZSCNT or ZSPOW) are used to solve the iterating equations via the nonlinear routine option IROUT (See namelist input sheet I-2). By this means, the user chooses the iteration method to be used.

At each iteration, the rub element physical forces at joint I (the P forces) must be found so that they can be plugged into the iterating equations. These forces are found in subroutine NLFORP. The next section details how we find these forces.

5.0 General Nonlinear Rub Element

5.1 Physical Force equations at Joint I

We now turn our attention to the equations for the rub element physical forces at joint I. These equations are nonlinear, both because of a cubic term and because of the dead band.

We define:

$P_{\ell,v,I}$ = Physical forces for the ℓ^{th} rub element in the vertical direction at joint I

$P_{\ell,H,I}$ = Physical force for the ℓ^{th} rub element in the horizontal direction at joint I

$\left|\Delta_\ell\right| = \sqrt{\left(\Delta X_{\ell,v}\right)^2+\left(\Delta X_{\ell,H}\right)^2}$ = Relative displacement magnitude for the ℓ th rub element.

$\Delta X_{\ell,v}$ = Relative displacement in the vertical direction for the ℓ^{th} rub element (that is, the vertical displacement at joint I minus that at joint J)

$\Delta X_{\ell,H}$ = Relative displacement in the horizontal direction for the ℓ^{th} rub element (that is, the horizontal displacement at joint I minus that at joint J)

$\Delta\dot{X}_{\ell,v}$ = Relative velocity in the vertical direction for the ℓ^{th} rub element

$\Delta\dot{X}_{\ell,H}$ = Relative velocity in the horizontal direction for the ℓ^{th} rub element

ϵ_0 = Dead band (this equals input variable DBAND on the type F input sheet)

K_ℓ = Linear radial spring constant factor for the ℓ^{th} rub element (this equals input variable SK on the type F input sheet)

μ_ℓ = Nonlinear radial spring constant factor for the ℓ^{th} rub element (this equals input variable AK on the type F input sheet)

C_ℓ = Damping coefficient for the ℓ^{th} rub element (this equals input variable CC on the type F input sheet)

We can write:

$$for\ \left|\Delta_\ell\right| \le \epsilon_0:\quad P_{\ell,v,I}=0\quad ;\quad P_{\ell,H,I}=0$$

$$for\ \left|\Delta_\ell\right| > \epsilon_0:\quad P_{\ell,v,I} = -K_\ell\Delta X_{\ell,v}\left(1-\frac{\epsilon_0}{\left|\Delta_\ell\right|}\right)\left[1+\mu_\ell\left(\left|\Delta_\ell\right|-\epsilon_0\right)^2\right]-C_\ell\,\Delta\dot{X}_{\ell,v} \qquad (30)$$

$$P_{\ell,H,I} = -K_\ell\Delta X_{\ell,H}\left(1-\frac{\epsilon_0}{\left|\Delta_\ell\right|}\right)\left[1+\mu_\ell\left(\left|\Delta_\ell\right|-\epsilon_0\right)^2\right]-C_\ell\,\Delta\dot{X}_{\ell,H} \qquad (31)$$

5.2 Harmonic Averaging

In order to find the $P^c_{\ell,v,I}$, $P^c_{\ell,H,I}$, $P^s_{\ell,v,I}$, and $P^s_{\ell,H,I}$ values to plug into iterating equations 20 through 23, we approximate the rub element physical forces at joint I with the expressions:

$$P_{\ell,v,I} = P^c_{\ell,v,I} \cos \omega t + P^s_{\ell,v,I} \sin \omega t \qquad (32)$$

$$P_{\ell,H,I} = P^c_{\ell,H,I} \cos \omega t + P^s_{\ell,H,I} \sin \omega t \qquad (33)$$

These expressions are not exact because, due to the nonlinearity and complexity of equations 30 and 31, higher order terms involving $\cos 2\omega t$, $\sin 2\omega t$, $\cos 3\omega t$, $\sin 3\omega t$, etc. would also be present. However, these higher order terms are neglected and only the first harmonic terms retained. Our problem then boils down to finding the values of $P^c_{\ell,v,I}$ $P^c_{\ell,H,I}$ $P^s_{\ell,v,I}$, and $P^s_{\ell,H,I}$. This is accomplished using the method of harmonic averaging.

Given a function f(t), the method of harmonic averaging involves integrating over a cycle as follows:

for the cos part: $\int_0^{2\pi/\omega} f(t) \cos \omega t \, dt$

for the sin part: $\int_0^{2\pi/\omega} f(t) \sin \omega t \, dt$

In order to perform the harmonic averaging, the following integral transformations will be helpful. The derivation of these integral transformations is straight forward but is fairly lengthy so is not included here.

For the expression:

$q(t) = a \cos \omega t + b \sin \omega t$

We have:

$$\int_0^{2\pi/\omega} q(t) \cos \omega t \, dt = \frac{\pi}{\omega} a \qquad (34)$$

$$\int_0^{2\pi/\omega} q(t) \sin \omega t \, dt = \frac{\pi}{\omega} b \qquad (35)$$

$$\int_0^{2\pi/\omega} \dot{q}(t) \cos \omega t \, dt = \pi b \qquad (36)$$

$$\int_0^{2\pi/\omega} \dot{q}(t) \sin \omega t \, dt = -\pi a \qquad (37)$$

$$\int_0^{2\pi/\omega} q^3(t) \cos \omega t \, dt = \frac{3\pi a\left(a^2+b^2\right)}{4\omega} \qquad (38)$$

$$\int_0^{2\pi/\omega} q^3(t) \sin \omega t \, dt = \frac{3\pi b\left(a^2+b^2\right)}{4\omega} \qquad (39)$$

For the pair of expressions:

$$q_1(t) = a\ cos\,\omega t + b\ sin\,\omega t$$

$$q_2(t) = c\ cos\,\omega t + d\ sin\,\omega t$$

we have:

$$\int_0^{2\pi/\omega} q_1(t)\ q_2^2(t) cos\,\omega t\,dt = \frac{\pi\left[a(d^2 + 3c^2) + 2bcd\right]}{4\omega} \qquad (40)$$

$$\int_0^{2\pi/\omega} q_1(t)\ q_2^2(t) sin\,\omega t\,dt = \frac{\pi\left[b(c^2 + 3d^2) + 2acd\right]}{4\omega} \qquad (41)$$

Note that the $P^c_{\ell,v,I}$, $P^c_{\ell,H,I}$, $P^s_{\ell,v,I}$, *and* $P^s_{\ell,H,I}$ quantities, which are found via harmonic averaging (except when there is no rub), are functions of the relative displacement components $\Delta X^c_{\ell,v}$, $\Delta X^c_{\ell,H}$, $\Delta X^s_{\ell,v}$, *and* $\Delta X^s_{\ell,H}$. The ΔX's are the unknowns in the iterating equations, and each iteration provides a new guess for the ΔX's. Thus, the $P^c_{\ell,v,I}$, $P^c_{\ell,H,I}$, $P^s_{\ell,v,I}$, and $P^s_{\ell,H,I}$ values change for each iteration, so the harmonic averaging must be done for each iteration.

If the equations are simple enough, closed form equations may be derived to perform the harmonic averaging (as is done for a continual rub with dead band equal to 0). If the equations are too complex to solve in closed form, numerical integration (using Simpson's rule) is performed instead (as is done for a continual rub with dead band not equal to 0 and for an intermittent rub). The advantage of using closed form equations, if possible, is that the closed form equations are more efficient and more exact than the numerical integration.

Further details of how the harmonic averaging is accomplished is contained in sections 5.3.2, 5.3.3, and 5.3.4.

5.3 Four Possible Rub Categories

Four possible rub categories are recognized by TETRA 2. These categories are no rub, continual rub with dead band equal to zero, continual rub with dead band greater than zero, and intermittent rub. The categories are illustrated in figure 5-1.

The TETRA 2 program determines which of the four categories apply by comparing the maximum and minimum rub element relative displacements (calculated using equations 24 and 25) and the rub element dead band (input variable DBAND on the type F input sheet). Note that this determination must be made for each rub element and at each iteration (since the calculated maximum and minimum relative displacement magnitudes change from iteration and iteration).

Different logic is used to calculate the rub element physical force components $P^c_{\ell,v,I}$, $P^c_{\ell,H,I}$, $P^s_{\ell,v,I}$, and $P^s_{\ell,H,I}$ depending on which category applies. The following sections detail the equations used for each of the four rub categories.

5.3.1 No Rub

If it is determined that a given rub element has no rub (see section 5.3), then the rub element physical forces must be zero.

Hence, the program sets:

$$P^c_{\ell,v,I} = 0$$

$$P^c_{\ell,H,I} = 0$$

$$P^s_{\ell,v,I} = 0$$

$$P^s_{\ell,H,I} = 0$$

and we're done.

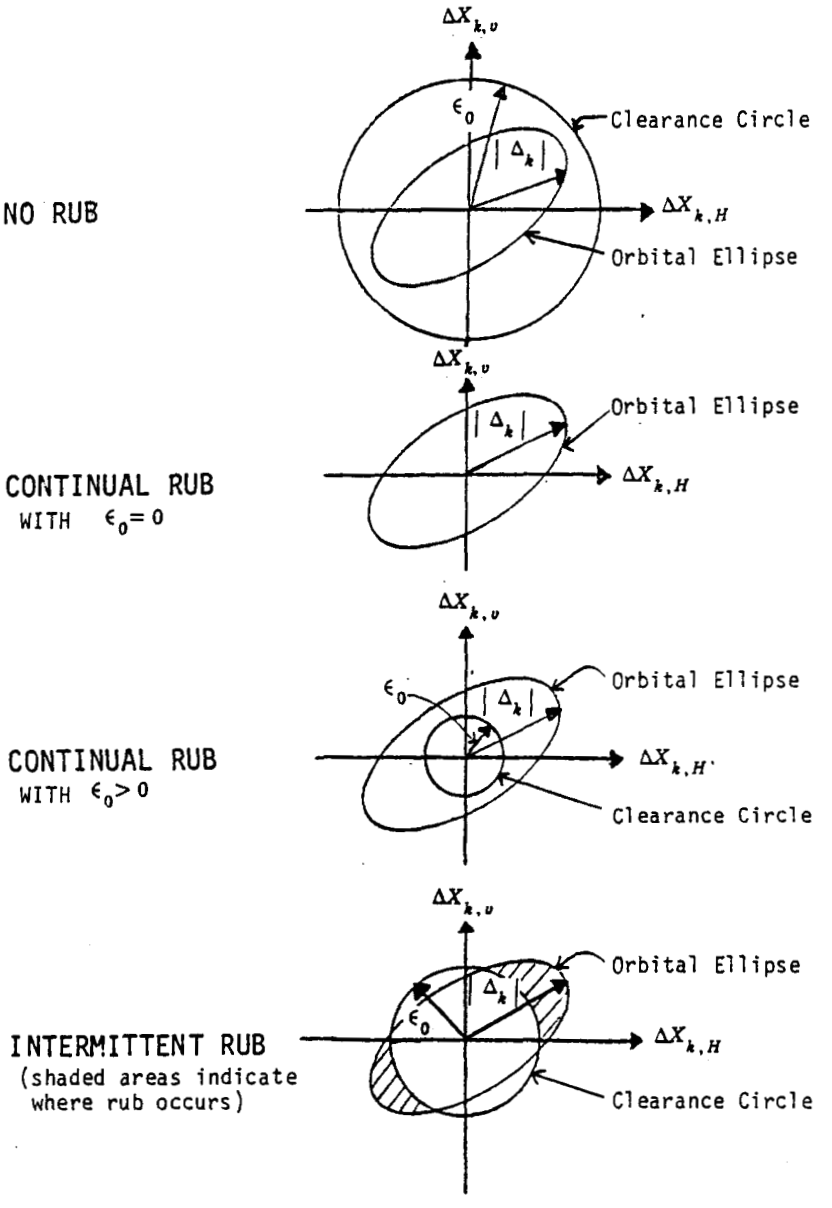

Nomenclature:

ϵ_0 = Dead Band

$|\Delta_k|$ = Relative displacement magnitude for the k'th rub element.

$\Delta X_{k,H}$ = Relative displacement of the k'th rub element in the horizontal direction

$\Delta X_{k,v}$ = Relative displacement of the k'th rub element in the vertical direction

FIGURE 5-1. FOUR POSSIBLE RUB CATEGORIES

5.3.2 Continual Rub with Dead Band Equal to Zero

If it is determined that we have a continual rub but the dead band equals 0 (see section 5.3), harmonic averaging is used to find $P^c_{\ell,v,I}$, $P^c_{\ell,H,I}$, $P^s_{\ell,v,I}$, and $P^s_{\ell,H,I}$. However, the equations simplify enough when the dead band equals 0 that we can derive closed form equations for $P^c_{\ell,v,I}$, $P^c_{\ell,H,I}$, $P^s_{\ell,v,I}$, and $P^s_{\ell,H,I}$, thus avoiding the less efficient process of integrating numerically. To find the desired closed form equations, we proceed as follows:

Setting $\epsilon_0 = 0$ in equations 30 and 31 we get:

$$P_{\ell,v,I} = -K_\ell \Delta X_{\ell,v} - K_\ell \mu_\ell \left(\Delta X_{\ell,v}\right)^3 - K_\ell \mu_\ell \, \Delta X_{\ell,v} \left(\Delta X_{\ell,H}\right)^2 - C_\ell \Delta \dot{X}_{\ell,v} \qquad (42)$$

$$P_{\ell,H,I} = -K_\ell \Delta X_{\ell,H} - K_\ell \mu_\ell \left(\Delta X_{\ell,H}\right)^3 - K_\ell \mu_\ell \, \Delta X_{\ell,H} \left(\Delta X_{\ell,v}\right)^2 - C_\ell \Delta \dot{X}_{\ell,H} \qquad (43)$$

Making use of the $\cos \omega t$ integral transformations (equations 34, 36, 38, and 40) equation 42 becomes:

$$\frac{\pi}{\omega} P^c_{\ell,v,I} = -\frac{\pi}{\omega} K_\ell \, \Delta X^c_{\ell,v} - \frac{3\pi}{4\omega} K_\ell \mu_\ell \, \Delta X^c_{\ell,v} \left[\left(\Delta X^c_{\ell,v}\right)^2 + \left(\Delta X^s_{\ell,v}\right)^2 \right]$$

$$- \frac{\pi}{4\omega} K_\ell \mu_\ell \left\{ \Delta X^c_{\ell,v} \left[\left(\Delta X^s_{\ell,H}\right)^2 + 3\left(\Delta X^c_{\ell,H}\right)^2 \right] + 2\Delta X^s_{\ell,v} \Delta X^c_{\ell,H} \, \Delta X^s_{\ell,H} \right\}$$

$$- \pi C_\ell \Delta X^s_{\ell,v}$$

Making use of the $\cos \omega t$ integral transformations (equations 34, 36, 38 and 40) equation 43 becomes:

$$\frac{\pi}{\omega} P^c_{\ell,H,I} = -\frac{\pi}{\omega} K_\ell \, \Delta X^c_{\ell,H} - \frac{3\pi}{4\omega} K_\ell \mu_\ell \, \Delta X^c_{\ell,H} \left[\left(\Delta X^c_{\ell,H}\right)^2 + \left(\Delta X^s_{\ell,H}\right)^2 \right]$$

$$- \frac{\pi}{4\omega} K_\ell \mu_\ell \left\{ \Delta X^c_{\ell,H} \left[\left(\Delta X^s_{\ell,v}\right)^2 + 3\left(\Delta X^c_{\ell,v}\right)^2 \right] + 2\Delta X^s_{\ell,H} \Delta X^c_{\ell,v} \, \Delta X^s_{\ell,v} \right\}$$

$$- \pi C_\ell \Delta X^s_{\ell,H}$$

Making use of the $\sin \omega t$ integral transformations (equations 35, 37, 39 and 41) equation 42 becomes:

$$\frac{\pi}{\omega} P^s_{\ell,v,I} = -\frac{\pi}{\omega} K_\ell \, \Delta X^s_{\ell,v} - \frac{3\pi}{4\omega} K_\ell \mu_\ell \, \Delta X^s_{\ell,v} \left[\left(\Delta X^c_{\ell,v}\right)^2 + \left(\Delta X^s_{\ell,v}\right)^2 \right]$$

$$- \frac{\pi}{4\omega} K_\ell \mu_\ell \left\{ \Delta X^s_{\ell,v} \left[\left(\Delta X^c_{\ell,H}\right)^2 + 3\left(\Delta X^s_{\ell,H}\right)^2 \right] + 2\Delta X^c_{\ell,v} \Delta X^c_{\ell,H} \, \Delta X^s_{\ell,H} \right\}$$

$$+ \pi C_\ell \Delta X^c_{\ell,v}$$

Making use of the $\sin \omega t$ integral transformations (equations 35, 37, 39 and 41) equation 43 becomes:

$$\frac{\pi}{\omega} P^s_{\ell,H,I} = -\frac{\pi}{\omega} K_\ell \Delta X^s_{\ell,H} - \frac{3\pi}{4\omega} K_\ell \mu_\ell \Delta X^s_{\ell,H} \left[\left(\Delta X^c_{\ell,H} \right)^2 + \left(\Delta X^s_{\ell,H} \right)^2 \right]$$

$$- \frac{\pi}{4\omega} K_\ell \mu_\ell \left\{ \Delta X^s_{\ell,H} \left[\left(\Delta X^c_{\ell,v} \right)^2 + 3 \left(\Delta X^s_{\ell,v} \right)^2 \right] + 2 \Delta X^c_{\ell,H} \Delta X^c_{\ell,v} \Delta X^s_{\ell,v} \right\}$$

$$+ \pi C_\ell \Delta X^c_{\ell,H}$$

Rewriting the last four equations we get:

$$P^c_{\ell,v,I} = -\frac{1}{4} K_\ell \mu_\ell \left[\Delta X^c_{\ell,v} \left\{ 3 \left(\Delta X^c_{\ell,v} \right)^2 + 3 \left(\Delta X^s_{\ell,v} \right)^2 + 3 \left(\Delta X^c_{\ell,H} \right)^2 + \left(\Delta X^s_{\ell,H} \right)^2 \right\} + 2 \Delta X^s_{\ell,v} \Delta X^c_{\ell,H} \Delta X^s_{\ell,H} \right]$$

$$- K_\ell \Delta X^c_{\ell,v} - \omega C_\ell \Delta X^s_{\ell,v}$$

$$P^c_{\ell,H,I} = -\frac{1}{4} K_\ell \mu_\ell \left[\Delta X^c_{\ell,H} \left\{ 3 \left(\Delta X^c_{\ell,v} \right)^2 + 3 \left(\Delta X^c_{\ell,H} \right)^2 + 3 \left(\Delta X^s_{\ell,H} \right)^2 + \left(\Delta X^s_{\ell,v} \right)^2 \right\} + 2 \Delta X^s_{\ell,H} \Delta X^c_{\ell,v} \Delta X^s_{\ell,v} \right]$$

$$- K_\ell \Delta X^c_{\ell,H} - \omega C_\ell \Delta X^s_{\ell,H}$$

$$P^s_{\ell,v,I} = -\frac{1}{4} K_\ell \mu_\ell \left[\Delta X^s_{\ell,v} \left\{ 3 \left(\Delta X^c_{\ell,v} \right)^2 + 3 \left(\Delta X^s_{\ell,v} \right)^2 + 3 \left(\Delta X^s_{\ell,H} \right)^2 + \left(\Delta X^c_{\ell,H} \right)^2 \right\} + 2 \Delta X^c_{\ell,v} \Delta X^c_{\ell,H} \Delta X^s_{\ell,H} \right]$$

$$- K_\ell \Delta X^s_{\ell,v} - \omega C_\ell \Delta X^c_{\ell,v}$$

$$P^s_{\ell,H,I} = -\frac{1}{4} K_\ell \mu_\ell \left[\Delta X^s_{\ell,H} \left\{ 3 \left(\Delta X^s_{\ell,v} \right)^2 + 3 \left(\Delta X^c_{\ell,H} \right)^2 + 3 \left(\Delta X^s_{\ell,H} \right)^2 + \left(\Delta X^c_{\ell,v} \right)^2 \right\} + 2 \Delta X^c_{\ell,H} \Delta X^c_{\ell,v} \Delta X^s_{\ell,v} \right]$$

$$- K_\ell \Delta X^s_{\ell,H} - \omega C_\ell \Delta X^c_{\ell,H}$$

5.3.3 Continual Rub with Dead Band Not Equal to Zero

If it is determined that we have a continual rub and the dead band does not equal 0 (see section 5.3), harmonic averaging is used to find $P^c_{\ell,v,I}$, $P^c_{\ell,H,I}$, $P^s_{\ell,v,I}$, and $P^s_{\ell,H,I}$. The equations for this category of rub are too complex to solve in closed form, so we must integrate numerically to find $P^c_{\ell,v,I}$, $P^c_{\ell,H,I}$, $P^s_{\ell,v,I}$, and $P^s_{\ell,H,I}$.

Using the integral transformation of equation 34 on the expression given in equation 32 we get:

$$P^c_{\ell,v,I} = \frac{\omega}{\pi} \int_0^{2\pi/\omega} P_{\ell,v,I} \cos \omega t \, dt$$

Using the integral transformation of equation 34 on the expression given in equation 33 we get:

$$P^{c}_{\ell,H,I} = \frac{\omega}{\pi} \int_{0}^{2\pi/\omega} P_{\ell,H,I} \cos \omega t \, dt$$

Using the integral transformation of equation 35 on the expression given in equation 32 we get:

$$P^{s}_{\ell,v,I} = \frac{\omega}{\pi} \int_{0}^{2\pi/\omega} P_{\ell,v,I} \sin \omega t \, dt$$

Using the integral transformation of equation 35 on the expression given in equation 33 we get:

$$P^{s}_{\ell,H,I} = \frac{\omega}{\pi} \int_{0}^{2\pi/\omega} P_{\ell,H,I} \sin \omega t \, dt$$

Substituting $\Psi = \omega t$, the preceding four equations can be rewritten:

$$P^{c}_{\ell,v,I} = \frac{1}{\pi} \int_{0}^{2\pi} P_{\ell,v,I} \cos \Psi \, d\Psi \qquad (44)$$

$$P^{c}_{\ell,H,I} = \frac{1}{\pi} \int_{0}^{2\pi} P_{\ell,H,I} \cos \Psi \, d\Psi \qquad (45)$$

$$P^{s}_{\ell,v,I} = \frac{1}{\pi} \int_{0}^{2\pi} P_{\ell,v,I} \sin \Psi \, d\Psi \qquad (46)$$

$$P^{s}_{\ell,H,I} = \frac{1}{\pi} \int_{0}^{2\pi} P_{\ell,H,I} \sin \Psi \, d\Psi \qquad (47)$$

For a continual rub, we note that the products $P_{\ell,v,I} \cos \Psi$, $P_{\ell,H,I} \cos \Psi$, $P_{\ell,v,I} \sin \Psi$, and $P_{\ell,H,I} \sin \Psi$ repeat themselves every 180°. Thus, we need only integrate between 0 and π and double the results as follows:

$$P^{c}_{\ell,v,I} = \frac{2}{\pi} \int_{0}^{\pi} P_{\ell,v,I} \cos \Psi \, d\Psi \qquad (48)$$

$$P^{c}_{\ell,H,I} = \frac{2}{\pi} \int_{0}^{\pi} P_{\ell,H,I} \cos \Psi \, d\Psi \qquad (49)$$

$$P^{s}_{\ell,v,I} = \frac{2}{\pi} \int_{0}^{\pi} P_{\ell,v,I} \sin \Psi \, d\Psi \qquad (50)$$

$$P^{s}_{\ell,H,I} = \frac{2}{\pi} \int_{0}^{\pi} P_{\ell,H,I} \sin \Psi \, d\Psi \qquad (51)$$

To perform the numerical integration, the integrals are divided into 10 subdivisions, with Ψ varying from 0 through π in steps of $\pi/10$. For each value of Ψ, the parameters $\Delta X_{\ell,v}$, $\Delta X_{\ell,H}$, $\Delta \dot{X}_{\ell,v}$, and $\Delta \dot{X}_{\ell,H}$ are calculated using the equations:

$$\Delta X_{\ell,v} = \Delta X^c_{\ell,v} \cos \omega t + \Delta X^s_{\ell,v} \sin \omega t$$

$$\Delta X_{\ell,H} = \Delta X^c_{\ell,H} \cos \omega t + \Delta X^s_{\ell,H} \sin \omega t$$

$$\Delta \dot{X}_{\ell,v} = \omega \Delta X^s_{\ell,v} \cos \omega t - \omega \Delta X^c_{\ell,v} \sin \omega t$$

$$\Delta \dot{X}_{\ell,H} = \omega \Delta X^s_{\ell,H} \cos \omega t - \omega \Delta X^c_{\ell,H} \sin \omega t$$

Substituting $\Psi = \omega t$ and rewriting:

$$\Delta X_{\ell,v} = \Delta X^c_{\ell,v} \cos \Psi + \Delta X^s_{\ell,v} \sin \Psi \qquad (52)$$

$$\Delta X_{\ell,H} = \Delta X^c_{\ell,H} \cos \Psi + \Delta X^s_{\ell,H} \sin \Psi \qquad (53)$$

$$\Delta \dot{X}_{\ell,v} = \omega\left(\Delta X^s_{\ell,v} \cos \Psi - \Delta X^c_{\ell,v} \sin \Psi \right) \qquad (54)$$

$$\Delta \dot{X}_{\ell,H} = \omega\left(\Delta X^s_{\ell,H} \cos \Psi - \Delta X^c_{\ell,H} \sin \Psi \right) \qquad (55)$$

where ω = forcing frequency, t = time, $\Psi = \omega t$, and the relative displacement components $\Delta X^c_{\ell,v}$, $\Delta X^c_{\ell,H}$, $\Delta X^s_{\ell,v}$ and $\Delta X^s_{\ell,H}$ are known because they are the guesses for the current iteration.

The $P_{\ell,v}$ and $P_{\ell,H}$ values are then calculated for each value of Ψ using equations 30 and 31.

Finally, knowing the $P_{\ell,v}$ and $P_{\ell,H}$ values for each value of Ψ between 0 and π (in steps of $\pi/10$), the values of the integrals in equations 48 through 51 are obtained using Simpson's rule.

5.3.4 Intermittent Rub

If it is determined that we have an intermittent rub (see section 5.3), harmonic averaging is used to find $P^c_{\ell,v,I}$, $P^c_{\ell,H,I}$, $P^s_{\ell,v,I}$, and $P^s_{\ell,H,I}$. Again, the equations for this category of rub are too complex to solve in closed form, so we must integrate numerically to find $P^c_{\ell,v,I}$, $P^c_{\ell,H,I}$, $P^s_{\ell,v,I}$, and $P^s_{\ell,H,I}$.

As for a continual rub with dead band equal to 0, the following equations are applicable (see equations 44-47 of section 5.3.3):

$$P^c_{\ell,v,I} = \frac{1}{\pi}\int_0^{2\pi} P_{\ell,v,I}\cos\Psi\, d\Psi$$

$$P^c_{\ell,H,I} = \frac{1}{\pi}\int_0^{2\pi} P_{\ell,H,I}\cos\Psi\, d\Psi$$

$$P^s_{\ell,v,I} = \frac{1}{\pi}\int_0^{2\pi} P_{\ell,v,I}\sin\Psi\, d\Psi$$

$$P^s_{\ell,H,I} = \frac{1}{\pi}\int_0^{2\pi} P_{\ell,H,I}\sin\Psi\, d\Psi$$

For an intermittent rub, the orbital ellipse intersects the clearance circle at four points (points A, B, C, and D in figure 5-2a). Rub element forces are present only for the two portions of the orbital ellipse that rub (between points A and B and between points C and D in figure 5-2a). Furthermore, the products $P_{\ell,v,I}\cos\Psi$, $P_{\ell,H,I}\cos\Psi$, $P_{\ell,v,I}\sin\Psi$, *and* $P_{\ell,H,I}\sin\Psi$ are the same for the two portions that rub (see sample $P_{\ell,v,I}\cos\Psi$ versus Ψ plot in figure 5-2b). Hence, we need only integrate over one of the two rub areas (say between points A and B) and double the result. Thus, the preceeding equations become:

$$P^c_{\ell,v,I} = \frac{2}{\pi}\int_{\Psi A}^{\Psi B} P_{\ell,v,I}\cos\Psi\, d\Psi \qquad (56)$$

$$P^c_{\ell,H,I} = \frac{2}{\pi}\int_{\Psi A}^{\Psi B} P_{\ell,H,I}\cos\Psi\, d\Psi \qquad (57)$$

$$P^s_{\ell,v,I} = \frac{2}{\pi}\int_{\Psi A}^{\Psi B} P_{\ell,v,I}\sin\Psi\, d\Psi \qquad (58)$$

$$P^s_{\ell,H,I} = \frac{2}{\pi}\int_{\Psi A}^{\Psi B} P_{\ell,H,I}\sin\Psi\, d\Psi \qquad (59)$$

where Ψ_A is the Ψ angle for point A and Ψ_B is the Ψ angle for point B.

Figure 5-2a. Orbital Ellipse and Clearance Circle
(Shaded areas indicate where rub occurs)

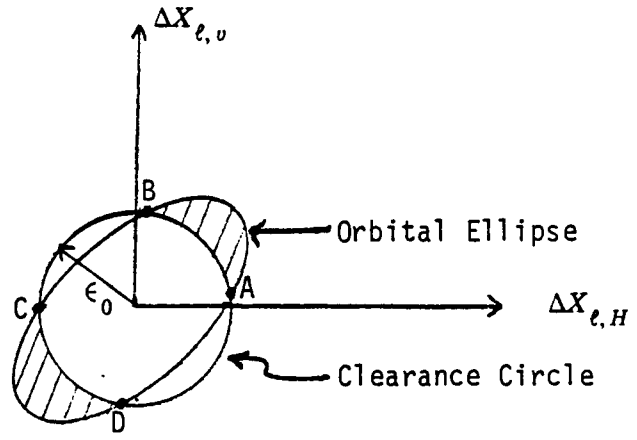

Figure 5-2b. Sample $P_{\ell,v,I}\cos\Psi$ Versus Ψ Plot

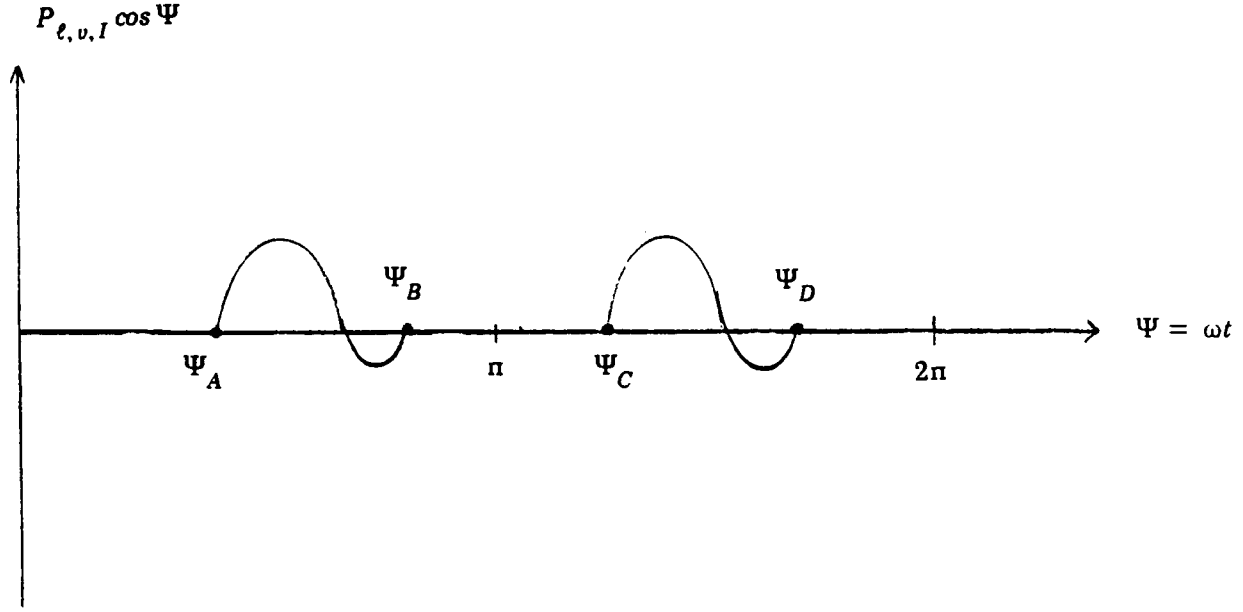

Figure 5-2. Intermittent Rub

To perform the numerical integration, the integrals are divided into 10 subdivisions, with Ψ varying from Ψ_A to Ψ_B in steps of $(\Psi_B - \Psi_A)/10$. The procedure is the same as for the continual rub with dead band not equal to 0. That is, first the $\Delta X_{\ell,v}$, $\Delta X_{\ell,H}$, $\Delta \dot{X}_{\ell,v}$, *and* $\Delta \dot{X}_{\ell,H}$ parameters are found for each Ψ value using equations 52 through 55. Then, the $P_{\ell,v}$ *and* $P_{\ell,H}$ values are calculated for each value of Ψ using equations 30 and 31. Finally, knowing the $P_{\ell,v}$ *and* $P_{\ell,H}$ values for each value of Ψ, the values of the integrals in equations 56 through 59 are calculated using Simpson's rule.

So far we have not covered how to find the Ψ_A *and* Ψ_B angles over which the integration is performed. This is explained in section 5.4.

5.4 Equations For the Intersection of the Orbital Ellipse and the Clearance Circle

For an intermittent rub, we must find the equations for the intersection of the orbital ellipse with the clearance circle. This is needed because we must numerically integrate over one of the two rub areas, and we must know the beginning angle Ψ_A and the ending angle Ψ_B for the integration (see section 5.3.4). We proceed as follows:

The equations for the orbital ellipse of a rub element are:

$$\Delta X_v = \Delta X_v^c \cos\Psi + \Delta X_v^s \sin\Psi \qquad (60)$$

$$\Delta X_H = \Delta X_H^c \cos\Psi + \Delta X_H^s \sin\Psi \qquad (61)$$

where $\Psi = \omega t$

Defining:

$$\Delta X_v^m = \sqrt{\left(\Delta X_v^c\right)^2 + \left(\Delta X_v^s\right)^2}$$

$$\Delta X_c^m = \sqrt{\left(\Delta X_H^c\right)^2 + \left(\Delta X_H^s\right)^2}$$

$$\Phi_v = \tan^{-1}\frac{\Delta X_v^s}{\Delta X_v^c}$$

$$\Phi_H = \tan^{-1}\frac{\Delta X_H^s}{\Delta X_H^c}$$

Equations 60 and 61 can then be written as:

$$\Delta X_v = \Delta X_v^m \cos\left(\Psi - \Phi_v\right) \qquad (62)$$

$$\Delta X_H = \Delta X_H^m \cos\left(\Psi - \Phi_H\right) \qquad (63)$$

For the four intersection points of the orbital ellipse with the clearance circle (whose radius ϵ_0 = the dead band) (see figure 5-2) we can write:

$$\left(\Delta X_v\right)^2 + \left(\Delta X_H\right)^2 = \left(\epsilon_0\right)^2 \qquad (64)$$

Plugging equations 62 and 63 into equation 64 we get:

$$\left(\Delta X_v^m\right)^2 \cos^2\left(\Psi - \Phi_v\right) + \left(\Delta X_H^m\right)^2 \cos^2\left(\Psi - \Phi_H\right) = \left(\epsilon_0\right)^2$$

Dividing through by ϵ_0^2 we get:

$$\left(\frac{\Delta X_v^m}{\epsilon_0}\right)^2 \cos^2\left(\Psi - \Phi_v\right) + \left(\frac{\Delta X_H^m}{\epsilon_0}\right)^2 \cos^2\left(\Psi - \Phi_H\right) = 1$$

Using a trigometric identity this becomes:

$$\left(\frac{\Delta X_v^m}{\epsilon_0}\right)^2\left(\frac{1 + \cos\left[2\left(\Psi - \Phi_v\right)\right]}{2}\right) + \left(\frac{\Delta X_H^m}{\epsilon_0}\right)^2\left(\frac{1 + \cos\left[2\left(\Psi - \Phi_H\right)\right]}{2}\right) = 1$$

Rearranging:

$$\frac{1}{2}\left[\left(\frac{\Delta X_v^m}{\epsilon_0}\right)^2 + \left(\frac{\Delta X_H^m}{\epsilon_0}\right)^2\right] + \frac{1}{2}\left(\frac{\Delta X_v^m}{\epsilon_0}\right)^2 \cos\left(2\Psi - 2\Phi_v\right) + \frac{1}{2}\left(\frac{\Delta X_H^m}{\epsilon_0}\right)^2 \cos\left(2\Psi - 2\Phi_H\right) = 1$$

Using another trigometric identity this becomes:

$$\frac{1}{2}\left[\left(\frac{\Delta X_v^m}{\epsilon_0}\right)^2 + \left(\frac{\Delta X_H^m}{\epsilon_0}\right)^2\right] + \frac{1}{2}\left(\frac{\Delta X_v^m}{\epsilon_0}\right)^2 \left(\cos 2\Psi \cos 2\Phi_v + \sin 2\Psi \sin 2\Phi_v\right)$$
$$+ \frac{1}{2}\left(\frac{\Delta X_H^m}{\epsilon_0}\right)^2 \left(\cos 2\Psi \cos 2\Phi_H + \sin 2\Psi \sin 2\Phi_H\right) = 1$$

Rearranging:

$$\frac{1}{2}\left[\left(\frac{\Delta X_v^m}{\epsilon_0}\right)^2 \cos 2\Phi_v + \left(\frac{\Delta X_H^m}{\epsilon_0}\right)^2 \cos 2\Phi_H\right] \cos 2\Psi$$
$$+ \frac{1}{2}\left[\left(\frac{\Delta X_v^m}{\epsilon_0}\right)^2 \sin 2\Phi_v + \left(\frac{\Delta X_H^m}{\epsilon_0}\right)^2 \sin 2\Phi_H\right] \sin 2\Psi = 1 - \frac{1}{2}\left[\left(\frac{\Delta X_v^m}{\epsilon_0}\right)^2 + \left(\frac{\Delta X_H^m}{\epsilon_0}\right)^2\right]$$

This can be rewritten:

$$A\cos 2\Psi + B\sin 2\Psi = C \qquad (65)$$

where

$$A = \frac{1}{2}\left[\left(\frac{\Delta X_v^m}{\epsilon_0}\right)^2 \cos 2\Phi_v + \left(\frac{\Delta X_H^m}{\epsilon_0}\right)^2 \cos 2\Phi_H\right]$$

$$B = \frac{1}{2}\left[\left(\frac{\Delta X_v^m}{\epsilon_0}\right)^2 \sin 2\Phi_v + \left(\frac{\Delta X_H^m}{\epsilon_0}\right)^2 \sin 2\Phi_H\right]$$

$$C = 1 - \frac{1}{2}\left[\left(\frac{\Delta X_v^m}{\epsilon_0}\right)^2 + \left(\frac{\Delta X_H^m}{\epsilon_0}\right)^2\right]$$

Defining:

$$\alpha = \tan^{-1}\frac{B}{A}$$

Equation 65 can be rewritten:

$$\sqrt{A^2 + B^2}\cos\left(2\Psi - \alpha\right) = C$$

from which we get:

$$2\Psi - \alpha = \cos^{-1}\left(\frac{C}{\sqrt{A^2 + B^2}}\right)$$

$$\Psi = \frac{\cos^{-1}\left(\frac{C}{\sqrt{A^2 + B^2}}\right)}{2} + \frac{\alpha}{2} \qquad (66)$$

Defining:

$$\theta = \cos^{-1}\left(\frac{C}{\sqrt{A^2 + B^2}}\right)$$

where:

$$0 \leq \theta \leq \pi$$

We can then list four possible values of the function:

$$\cos^{-1}\left(\frac{C}{\sqrt{A^2+B^2}}\right)$$

as follows:

$$\cos^{-1}\left(\frac{C}{\sqrt{A^2+B^2}}\right) = \theta$$

$$\cos^{-1}\left(\frac{C}{\sqrt{A^2+B^2}}\right) = 2\pi - \theta$$

$$\cos^{-1}\left(\frac{C}{\sqrt{A^2+B^2}}\right) = 2\pi + \theta$$

$$\cos^{-1}\left(\frac{C}{\sqrt{A^2+B^2}}\right) = 4\pi - \theta$$

Plugging these four possible values into equation 66 we get:

$$\Psi_1 = \frac{\theta}{2} + \frac{\alpha}{2}$$

$$\Psi_2 = \pi - \frac{\theta}{2} + \frac{\alpha}{2}$$

$$\Psi_3 = \pi + \frac{\theta}{2} + \frac{\alpha}{2}$$

$$\Psi_4 = 2\pi - \frac{\theta}{2} + \frac{\alpha}{2}$$

The preceding equations give the Ψ angles for the four intersection points of the orbital ellipse with clearance circle. As discussed in section 5.3.4, we numerically integrate over one of the two rub areas, then double the result. However, given the four intersection points, there is the possibility that the rub areas are between points 1 and 2 and between points 3 and 4, and there is also the possibility that the rub areas are between points 2 and 3 and between points 4 and 1 (see figure 5-3). To find which of these two possibilities apply, we first calculate the Ψ angle at point 1.5, which is half way between points 1 and 2:

$$\Psi_{1.5} = \frac{\Psi_1 + \Psi_2}{2} = \pi + \frac{\alpha}{2}$$

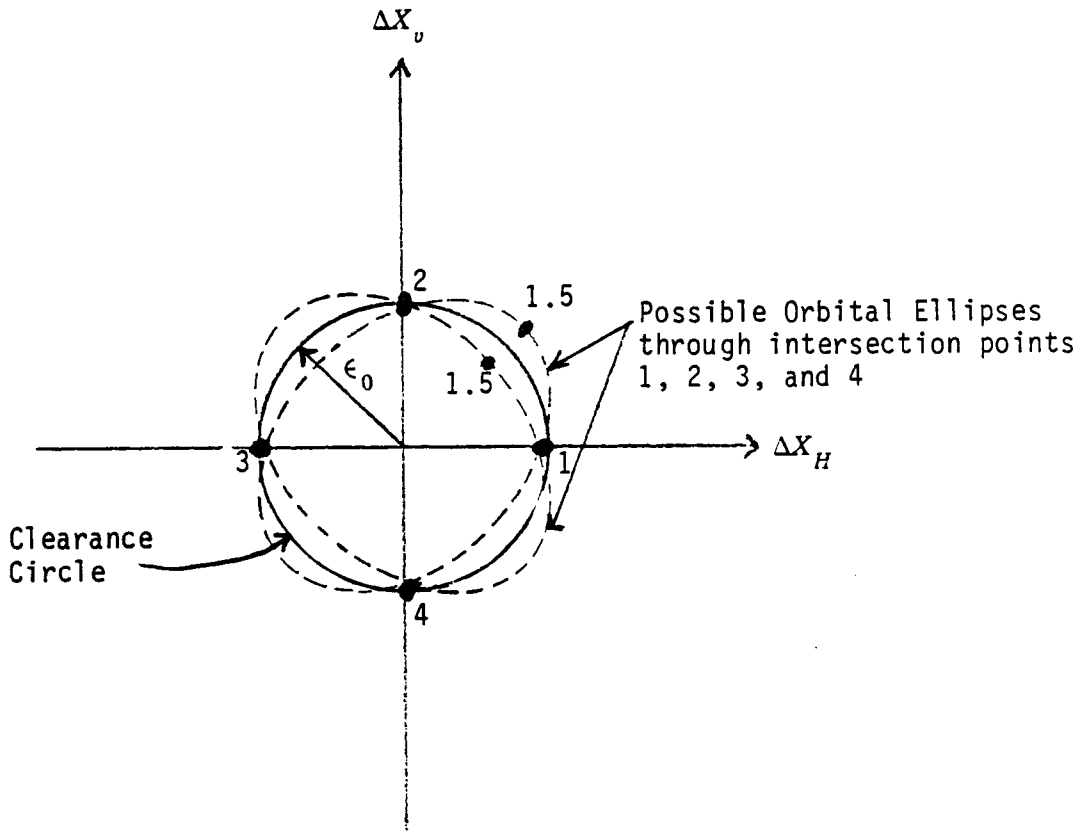

Figure 5-3. Orbital Ellipse Possibilities For An Intermittent Rub

We then calculate the radius at point 1.5 as follows:

$$R_{1.5} = \sqrt{\left(\Delta X_v\right)^2 + \left(\Delta X_H\right)^2}$$

$$R_{1.5} = \sqrt{\left(\Delta X_v^c \cos \Psi_{1.5} + \Delta X_v^s \sin \Psi_{1.5}\right)^2 + \left(\Delta X_H^c \cos \Psi_{1.5} + \Delta X_H^s \sin \Psi_{1.5}\right)^2}$$

If the radius at point 1.5 is greater than the dead band, then the rub areas must be between points 1 and 2 and between points 3 and 4. If this is the case, we numerically integrate between points:

$$\Psi_A = \Psi_1 \quad and \quad \Psi_B = \Psi_2$$

as detailed in section 5.3.4.

However, if the radius at point 1.5 is less than the dead band, then the rub areas must be between points 2 and 3 and between points 4 and 1. If this is the case, we numerically integrate between points:

$$\Psi_A = \Psi_2 \quad and \quad \Psi_B = \Psi_3$$

as detailed in section 5.3.4.

5.5 Equations For the Maximum and Minimum Rub Element Harmonically Averaged Force Magnitude

As noted in section 5.2, the rub element physical forces are expressed as:

$$P_{\ell,v,I} = P^{c}_{\ell,v,I} \cos \omega t + P^{s}_{\ell,v,I} \sin \omega t$$

$$P_{\ell,H,I} = P^{c}_{\ell,H,I} \cos \omega t + P^{s}_{\ell,H,I} \sin \omega t$$

where $P^{c}_{\ell,v,I}$ $P^{c}_{\ell,H,I}$, $P^{s}_{\ell,v,I}$, *and* $P^{s}_{\ell,H,I}$ are found using harmonic averaging.

We next define:

$$P^{m}_{\ell,v,I} = \sqrt{\left(P^{c}_{\ell,v,I}\right)^2 + \left(P^{s}_{\ell,v,I}\right)^2}$$

$$P^{m}_{\ell,H,I} = \sqrt{\left(P^{c}_{\ell,H,I}\right)^2 + \left(P^{s}_{\ell,H,I}\right)^2}$$

$$\Phi_{v} = tan^{-1} \frac{P^{s}_{\ell,v,I}}{P^{c}_{\ell,v,I}}$$

$$\Phi_{H} = tan^{-1} \frac{P^{s}_{\ell,H,I}}{P^{c}_{\ell,H,I}}$$

$$\Phi = \Phi_{v} - \Phi_{H}$$

F_{max} = Maximum rub element harmonically averaged force magnitude

F_{min} = Minimum rub element harmonically averaged force magnitude

It can be shown (though the derivation is lengthy, so we skip it here):

$$F_{max} = \sqrt{\frac{\left(P^m_{\ell,v,I}\right)^2 + \left(P^m_{\ell,H,I}\right)^2}{2} + \frac{1}{2}\sqrt{\left(P^m_{\ell,v,I}\right)^4 + \left(P^m_{\ell,H,I}\right)^4 + 2\left(P^m_{\ell,v,I}\right)^2\left(P^m_{\ell,H,I}\right)^2 \cos 2\Phi}}$$

$$F_{min} = \sqrt{\frac{\left(P^m_{\ell,v,I}\right)^2 + \left(P^m_{\ell,H,I}\right)^2}{2} - \frac{1}{2}\sqrt{\left(P^m_{\ell,v,I}\right)^4 + \left(P^m_{\ell,H,I}\right)^4 + 2\left(P^m_{\ell,v,I}\right)^2\left(P^m_{\ell,H,I}\right)^2 \cos 2\Phi}}$$

Note that these equations are similar in form to the equations for the maximum and minimum relative displacement magnitudes given in section 4.5.3.

6.0 Generalized Displacements and Generalized Velocities

6.1 Generalized Displacements

The generalized displacements can be written in terms of the cos and sin components as follows:

$$Z_k = Z_k^c \cos \omega t + Z_k^s \sin \omega t \qquad (67)$$

where:

Z_k = generalized displacement for global mode k

Z_k^c = amplitude of the cos component of the generalized displacement mode k

Z_k^s = amplitude of the sin component of the generalized displacement mode k

ω = steady state forcing frequency

t = time

The amplitude of the cos and sin component of the generalized displacement for each mode is calculated using the method outlined in section 4.5.1. The generalized displacements can also be expressed in terms of the magnitude and phase angle as follows:

$$Z_k = Z_k^m \cos\left(\omega t - \zeta_k\right)$$

where:

$$Z_k^m = \sqrt{\left(Z_k^c\right)^2 + \left(Z_k^s\right)^2}$$

$$\zeta_k = \tan^{-1}\left(\frac{Z_k^s}{Z_k^c}\right)$$

For each forcing frequency, the generalized displacements are found as outlined above and in section 4.5.1. The generalized displacements are then used to calculate the physical quantities (physical displacements, physical velocities, physical connecting element forces, etc.) as outlined in section 7 which follows. It is normally the physical quantities that the user is interested in rather than the generalized values. For this reason, printout of the generalized displacements is omitted if the user requests the short or the standard form of the output (see printout option IOUT on the type A input sheet). Printout of the generalized displacements (cos components, sin components, magnitudes, and phase angles) is included if the user requests the long form of the printed output.

6.2 Generalized Velocities

In a manner similar to that for the generalized displacements of the preceeding section, the generalized velocities can be expressed in terms of the cos and sin components as follows:

$$ZV_k = ZV_k^c \cos \omega t + ZV_k^s \sin \omega t$$

where:

ZV_k = generalized velocity for mode k

By differentiating equation 67, we can express the amplitudes of the cos and sin components of the generalized velocities in terms of the generalized displacements found via the method of the preceeding section as follows:

$$ZV_k^c = \omega Z_k^s$$

$$ZV_k^s = -\omega Z_k^c$$

7.0 Equations For the Physical Quantities

Once the generalized displacements and generalized velocities have been found, as outlined in section 6, they are used to calculate the physical quantities. The physical quantities are the last things calculated for each forced frequency solution. The following sections detail how the physical quantities are calculated.

7.1 Physical Displacements, Velocities, and Modal Forces at the Points

The physical displacement can be written in terms of the cos and sin components as follows:

$$X_{ij} = X^c_{ij} \cos \omega t + X^s_{ij} \sin \omega t$$

where:

X_{ij} = physical displacement for point i in direction j

The amplitude of the cos and sin components of the physical displacement is found by summing over the modes as follows:

$$X^c_{ij} = \sum_{k=1}^{n} \Phi^x_{ijk} Z^c_k$$

$$X^s_{ij} = \sum_{k=1}^{n} \Phi^x_{ijk} Z^s_k$$

where:

Φ^x_{ijk} = displacement mode shape for point i, direction j, and mode k

Z^c_k = amplitude of the cos component of the generalized displacement for mode k (see section 6.1)

Z^s_k = amplitude of the sin component of the generalized displacement for mode k (see section 6.1)

Similarly, the physical velocity can be written in terms of the cos and sin components as follows:

$$V_{ij} = V^c_{ij} \cos \omega t + V^s_{ij} \sin \omega t$$

where:

V_{ij} = physical velocity for point i in direction j

The amplitude of the cos and sin components of the physical velocity is found by summing over the modes as follows:

$$V_{ij}^{c} = \sum_{k=1}^{n} \Phi_{ijk}^{x} ZV_{k}^{c}$$

$$V_{ij}^{s} = \sum_{k=1}^{n} \Phi_{ijk}^{x} ZV_{k}^{s}$$

where:

ZV_k^c = amplitude of the cos component of the generalized velocity for mode k (see section 6.2)

ZV_k^s = amplitude of the sin component of the generalized velocity for mode k (see section 6.2)

Similarly, the modal force can be written in terms of the cos and sin components as follows:

$$F_{ij} = F_{ij}^{c} \cos \omega t + F_{ij}^{s} \sin \omega t$$

where:

F_{ij} = modal force for point i in direction j

The amplitude of the cos and sin components of the modal force is found by summing over the modes as follows:

$$F_{ij}^{c} = \sum_{k=1}^{n} \Phi_{ijk}^{f} Z_{k}^{c}$$

$$F_{ij}^{s} = \sum_{k=1}^{n} \Phi_{ijk}^{f} Z_{k}^{s}$$

where:

Φ_{ijk}^{f} = force mode shape for point i, direction j, and mode k

Note that the physical displacements and physical velocities are calculated using the displacement mode shapes, while the modal forces are calculated using the force mode shapes. For the flexible vertical and horizontal plane subsystems, the displacement mode shapes are the translation and slope, while the force mode shapes are the shear and moment as entered on input sheet C-3.

So far we have expressed the physical displacements, physical velocities, and modal forces in terms of the cos and sin components. These quantities can also be expressed in terms of the magnitude and phase angle as follows:

$$X_{ij} = X_{ij}^m \cos\left(\omega t - \zeta_{ij}^x\right)$$

$$V_{ij} = V_{ij}^m \cos\left(\omega t - \zeta_{ij}^v\right)$$

$$F_{ij} = F_{ij}^m \cos\left(\omega t - \zeta_{ij}^f\right)$$

where:

$$X_{ij}^m = \sqrt{\left(X_{ij}^c\right)^2 + \left(X_{ij}^s\right)^2}$$

$$\zeta_{ij}^x = \tan^{-1}\left(\frac{X_{ij}^s}{X_{ij}^c}\right)$$

$$V_{ij}^m = \sqrt{\left(V_{ij}^c\right)^2 + \left(V_{ij}^s\right)^2}$$

$$\zeta_{ij}^v = \tan^{-1}\left(\frac{V_{ij}^s}{V_{ij}^c}\right)$$

$$F_{ij}^m = \sqrt{\left(F_{ij}^c\right)^2 + \left(F_{ij}^s\right)^2}$$

$$\zeta_{ij}^f = \tan^{-1}\left(\frac{F_{ij}^s}{F_{ij}^c}\right)$$

Usually, the user is primarily interested in the magnitudes of the quantities. For this reason, it is the magnitudes and phase angles of these quantities, rather than the cos and sin components, that are printed out and written to the output plot file. An exception to this is that the cos and sin components are also printed out if the long form of the printed output is requested via input variable IOUT on type A input sheet.

7.2 Physical Connecting and Gyroscopic Element Forces

TETRA 2 has capability for six different types of physical connecting elements: type 1 (general spring-damper elements), type 2 (link elements), type 3 (rub elements), type 4 (engine support-links elements), type 5 (uncoupled point spring-damper elements), and type 6 (squeeze film damper elements). The first five types can be used for either transient or steady state analyses, while the type 6 (squeeze film damper elements) can be used only for transient analyses. In addition, TETRA 2 accounts for gyroscopic forces acting on a rotor by means of a gyroscopic element, which can be used for either transient or steady state analyses. Although not a physical connecting element, the gyroscopic element is classified as an element because gyroscopic forces are calculated very similarly to the damping forces of the physical connecting elements. This section concerns itself only with the element forces for steady state analysis runs, since the element forces for transient analysis runs were covered in reference 1 and reference 3.

The physical connecting or gyroscopic element force can be written in terms of the cos and sin components as follows:

$$F_{ijk} = F^c_{ijk} \cos \omega t + F^s_{ijk} \sin \omega t$$

where:

F_{ijk} = force that physical connecting or gyroscopic element k exerts on the engine components or ground for point i and direction j

F^c_{ijk} = amplitude of the cos component of the force that physical connecting or gyroscopic element k exerts on the engine component or ground for point i and direction j

F^s_{ijk} = amplitude of the sin component of the force that physical connecting or gyroscopic element k exerts on the engine component or ground for point i and direction j

The amplitude of the cos and sin components of the force that the element exerts on the engine component or ground is calculated very differently for the nonlinear type 3 physical connecting element (rub element) than for the other elements. For the rub elements, these are calculated using harmonic averaging (except when the dead band has not been exceeded so that the rub element forces are 0) as detailed in section 5. For joint I of the rub element, F^c_{ijk} in the above equation is the same as the variables $P^c_{\ell vI}$ (for the vertical direction) and $P^c_{\ell HI}$ (for the horizontal direction) from section 5. Likewise, F^c_{ijk} is the same as $P^s_{\ell vI}$ (for the vertical direction) and $P^s_{\ell HI}$ (for the horizontal direction) from section 5. The forces at joint J of the rub element are simply the negative of the forces at joint I of the rub element.

For the other elements, on the other hand, the F^c_{ijk} and F^s_{ijk} are calculated using the physical displacements and/or physical velocities at the joints of the element (the X^c_{ij}, X^s_{ij}, V^c_{ij}, *and* V^s_{ij} that were found in section 7.1) and data

pertaining to the stiffness and damping of the element. Just what stiffness and damping data is used along with the physical displacements and/or physical velocities to calculate the element forces depends on the type of physical connecting element and the user input options which were chosen. Input stiffness matrix definition or input stiffness coefficients are used obtain the stiffness of the element. The damping of the element may be obtained by input damping matrix definition, input damping coefficients, or may be calculated using an input Q-factor and a frequency. The frequency used along with the input Q-factor to calculate the damping may either be input (non-structural damping), or the steady state forcing frequency or independent rotor speed may be used for this frequency (structural damping). In the case of the gyroscopic element, the polar moment of inertia and the rotor speed are used to calculate the damping. See reference 1 for more details about the physical connecting and gyroscopic elements.

The physical connecting and gyroscopic element forces may also be expressed in terms of magnitude and phase angle as follows:

$$F_{ijk} = F^{m}_{ijk} \cos\left(\omega t - \zeta_{ijk}\right)$$

where:

$$F^{m}_{ijk} = \sqrt{\left(F^{c}_{ijk}\right)^2 + \left(F^{s}_{ijk}\right)^2}$$

$$\zeta_{ijk} = \tan^{-1}\left(\frac{F^{s}_{ijk}}{F^{c}_{ijk}}\right)$$

Usually, the user is interested primarily in the magnitude of the element forces. For this reason, it is the magnitudes and phase angles of these quantities, rather than the cos and sin components, that are printed out and written to the output plot file. An exception to this is that the cos and sin components are also printed out if the long form of the printed output is requested via input variable IOUT on the type A input sheet.

7.3 Flexible Bladed Disk Displacements and Stresses

For each flexible bladed disk, two modes are considered. These modes are the horizontal nodal diameter mode (referred to as mode P) and the vertical nodal diameter mode (referred to as mode Q). In a given TETRA model, there can be a maximum of two flexible bladed disks, and these flexible bladed disks must be located on the same rotor. See reference 2 for a detailed discussion of the two nodal diameter modes and flexible bladed disks in general.

The equations for the displacements and stresses at a local point on flexible bladed disk number 1 or 2 (from reference 2 page 11 and 21) are:

$$U = \overline{U}\left(P \sin \Psi + Q \cos \Psi\right) \tag{68}$$

$$V = \overline{V}\left(P \sin \Psi + Q \cos \Psi\right) \tag{69}$$

$$S_1 = \overline{S_1}\left(P \sin \Psi + Q \cos \Psi\right) \tag{70}$$

$$S_2 = \overline{S_2}\left(P \sin \Psi + Q \cos \Psi\right) \tag{71}$$

$$S_3 = \overline{S_3}\left(P \sin \Psi + Q \cos \Psi\right) \tag{72}$$

where:

U = tangential displacement of the local point on the flexible bladed disk

$\overline{U}$ = input static (zero speed) mode shape for tangential translation of the local point on the flexible bladed disk

V = axial displacement of the local point on the flexible bladed disk

$\overline{V}$ = input static (zero speed) mode shape for axial translation of the local point on the flexible bladed disk

S_1 = first stress component of the local point on the flexible bladed disk

$\overline{S_1}$ = input modal stress for the first stress component of the local point on the flexible bladed disk

S_2 = second stress component of the local point on the flexible bladed disk

$\overline{S_2}$ = input modal stress for the second stress component of the local point on the flexible bladed disk

S_3 = third stress component of the local point on the flexible bladed disk

$\overline{S_3}$ = input modal stress for the third stress component of the local point on the flexible bladed disk

P = generalized displacement for the horizontal nodal diameter mode of the flexible bladed disk

Q = generalized displacement for the vertical nodal diameter mode of the flexible bladed disk

Ψ = polar angle of the local point on the flexible bladed disk

The polar angle of the local point on the flexible bladed disk is found from:

$$\Psi = \Omega t + \Phi$$

where:

Ω = flexible bladed disk rotor speed

t = time

Φ = input polar angle of the local point on the flexible bladed disk relative to the flexible bladed disk reference diameter (see input sheet C-15)

Also, for a steady state analysis run we can express the generalized displacement of the P and Q modes in terms of magnitude and phase angle as follows:

$$P = P^m \cos\left(\omega t - \zeta_p\right)$$

$$Q = Q^m \cos\left(\omega t - \zeta_q\right)$$

where the magnitude and phase angle for the P and Q modes are calculated just like those of the other generalized displacements (see section 6.1).

Plugging the expressions for Ψ, P, and Q into equations 68 through 72, we arrive at fairly complex expressions for the displacements and stresses at a local point on a flexible bladed disk:

$$U = \overline{U}\left[P^m \cos\left(\omega t - \zeta_p\right)\sin\left(\Omega t + \Phi\right) + Q^m \cos\left(\omega t - \zeta_q\right)\cos\left(\Omega t + \Phi\right)\right]$$

$$V = \overline{V}\left[P^m \cos\left(\omega t - \zeta_p\right)\sin\left(\Omega t + \Phi\right) + Q^m \cos\left(\omega t - \zeta_q\right)\cos\left(\Omega t + \Phi\right)\right]$$

$$S_1 = \overline{S_1}\left[P^m \cos\left(\omega t - \zeta_p\right)\sin\left(\Omega t + \Phi\right) + Q^m \cos\left(\omega t - \zeta_q\right)\cos\left(\Omega t + \Phi\right)\right]$$

$$S_2 = \overline{S_2}\left[P^m \cos\left(\omega t - \zeta_p\right)\sin\left(\Omega t + \Phi\right) + Q^m \cos\left(\omega t - \zeta_q\right)\cos\left(\Omega t + \Phi\right)\right]$$

$$S_3 = \overline{S_3}\left[P^m \cos\left(\omega t - \zeta_p\right)\sin\left(\Omega t + \Phi\right) + Q^m \cos\left(\omega t - \zeta_q\right)\cos\left(\Omega t + \Phi\right)\right]$$

We can define the magnitude portions of these expressions as follows:

$$U_p^m = \overline{U}\, P^m$$
$$U_q^m = \overline{U}\, Q^m$$
$$V_p^m = \overline{V}\, P^m$$
$$V_q^m = \overline{V}\, Q^m$$
$$S_{1p}^m = \overline{S_1}\, P^m$$
$$S_{1q}^m = \overline{S_1}\, Q^m$$
$$S_{2p}^m = \overline{S_2}\, P^m$$
$$S_{2q}^m = \overline{S_2}\, Q^m$$
$$S_{3p}^m = \overline{S_3}\, P^m$$
$$S_{3q}^m = \overline{S_3}\, Q^m$$

It is these magnitudes that are printed out and written onto the plot file for a steady state analysis run.

Substituting the magnitude quantities into the expressions for the displacements and stresses at a local point on a flexible bladed disk we get:

$$U = U_p^m \cos\left(\omega t - \zeta_p\right) \sin\left(\Omega t + \Phi\right) + U_q^m \cos\left(\omega t - \zeta_p\right) \cos\left(\Omega t + \Phi\right)$$

$$V = V_p^m \cos\left(\omega t - \zeta_p\right) \sin\left(\Omega t + \Phi\right) + V_q^m \cos\left(\omega t - \zeta_p\right) \cos\left(\Omega t + \Phi\right)$$

$$S_1 = S_{1p}^m \cos\left(\omega t - \zeta_p\right) \sin\left(\Omega t + \Phi\right) + S_{1q}^m \cos\left(\omega t - \zeta_p\right) \cos\left(\Omega t + \Phi\right)$$

$$S_2 = S_{2p}^m \cos\left(\omega t - \zeta_p\right) \sin\left(\Omega t + \Phi\right) + S_{2q}^m \cos\left(\omega t - \zeta_p\right) \cos\left(\Omega t + \Phi\right)$$

$$S_3 = S_{3p}^m \cos\left(\omega t - \zeta_p\right) \sin\left(\Omega t + \Phi\right) + S_{3q}^m \cos\left(\omega t - \zeta_p\right) \cos\left(\Omega t + \Phi\right)$$

8.0 CONCLUDING REMARKS FOR VOLUME 1.

This volume documents the methodology for the steady state solution incorporated in TETRA 2. It is written to permit a straightforward understanding of its developments from the essentials of the theory, to the actual applications to engine dynamics and to the programmed working equations. These also include the treatment of nonlinear elements and the case of the intermittent rubs.

It is intended that this volume should be a self contained description of the entire theory, as well as an accompaniment to the second volume.

Volume 2 is the user's manual which contains both program input/output description and the trial or sample illustrative cases. The latter is a documentation of the progressive steps that were taken to debug and check the program, from simple degenerate cases to the twin spool engine model. This volume is also intended to be a self contained user's manual. However, to those interested in cross-checking program with theory, Volume 1 will be necessary.

9.0 REFERENCES

1. Gallardo, V. et al, 'Blade Loss Transient Analysis', Task II and Task III, NASA CR-165373, Volumes II and III, June 1981.

2. Gallardo, V. and Black, G. et al, 'Blade Loss Transient Dynamic Analysis with Flexible Bladed Disk', NASA CR-168176, April 1983

3. Ghaby, R.A., 'The Transient/Nonlinear Vibration of Gas Turbine Jet Engines With Squeeze Film Dampers Due To Blade Loss', Master's Thesis, Department of Mechanical and Aerospace Engineering, Case Western Reserve University, Cleveland, Ohio, May 1984.

4. Hurty, W.C., 'Dynamic Analysis of Structural Systems Using Component Modes', AIAA Journal, Vol. 3, April 1963.

5. Stallone, M.J. and Gallardo, V.C. et al, 'Blade Loss Transient Dynamic Analysis of Turbomachinery' AIAA Journal Vol. 21, No. 8, August, 1983.

6. Leimanis, E. and Minorsky, N., 'Dynamics and Nonlinear Mechanics', Section 2: The Theory of Oscillations (A Survey of Nonlinear Methods), Surveys in Applied Mathematics II, John Wiley and Sons, N.Y., N.Y., 1958.

7. Dinca, F. and Teodosiu, C. 'Nonlinear and Random Vibrations', Academic Press, N.Y., N.Y., 1973.

8. Silijak, D., 'Nonlinear Systems', John Wiley and Sons, Inc., N.Y., N.Y., 1969.

9. Kryloff, N. and Bogolinboff, N., 'Introduction to Nonlinear Mechanics', English Version by S. Lefschetz, Princeton University Press, Princeton, N.J. 1943; also see: 6.0, 7.0.

10. Minorsky, N., 'Introduction to Nonlinear Mechanics', J.W. Edwards, Ann Arbor, MI., 1946.

11. Tongue, B.H and Dowell, E.H., 'Component Mode Analysis of Nonlinear, Nonconservative Systems', Journal of Applied Mechanics, Vol. 50, March 1983 (PP 204).

	Mail Stop	Copies
NASA Lewis Research Center 21000 Brookpark Road Cleveland, OH 44135		
Attn: Contracting Officer	500-305	1
Technical Report Control	5-5	1
Technology Utilization Office	3-19	1
AFSC Liaison Office	501-3	1
Structures Div. Contract File	49-6	1
Library	60-3	1
D. W. Drier	86-2	1
E. J. Hronek	86-2	1
Charles Lawrence	23-3	1
James D. McAleese	500-120	1
Lester D. Nichols	49-6	1
Daniel J. Gauntner	49-8	1
Louis J. Kiraly	23-3	1
Robert E. Kielb	23-3	1
Albert F. Kascak	23-3	1
David P. Fleming	23-3	1
Gerald V. Brown	23-3	1
Case Western Reserve University Mech. and Aero. Cleveland, OH 44106		
Attn: Professor Maurice Adams		1
Headquarters National Aeronautics & Space Administration Washington, DC 10546		
Attn: NHS-22/Library		2
RTM-6/S. Venneri		2
NASA Ames Research Center Moffett Field, CA 94035		
Attn: Library	202-3	1
NASA Goddard Space Flight Center Greenbelt, MD 20771		
Attn: 252/Library		1
NASA John F. Kennedy Space Center Kennedy Space Center, FL 32931		
Attn: Library	AD-L50-1	1
NASA Langley Research Center Hampton, VA 233365		
Attn: Library	185	2
NASA Lyndon B. Johnson Space Center Houston, TX 77001		
Attn: JM6/Library		1

NASA George C. Marshall Space Flight Center
Marshall Space Flight Center, AL 35812
Attn: AS61/Library 1

Jet Propulsion Laboratory
4000 Oak Groove Drive
Pasadena, CA 91103
Attn: Library 1

NASA S&T Info Facility
P. O. Box 8757
Baltimore-Washington Int. Airport, MD 21240
Attn: Acquisition Dept. 1

Air Force System Command
Aeronautical System Div.
Wright-Patterson AFB, OH 45433
Attn: Library 1
C. W. Cowie 1

Air Force Wright Aeronautical Lab.
Wright-Patterson AFB, OH 45433
Attn: I. Gershan 1
L. Bailey 1

Aerospace Corporation
2400 E. El Segundo Blvd.
Los Angeles, CA 90045
Attn: Library-Documents 1

Air Force Office of Scientific Research
Washington, DC 20333
Attn: Library 1

Department of the Army
U. S. Army Material Command
Washington, DC 20315
Attn: AMCRD-RC 1

U. S. Army Ballistics Research Lab.
Aberdeen Proving Ground, MD 21005
Attn: Dr. Donald F. Haskel
DRXBR-BM 1

Army Materials & Mechanics Research Center
Watertown, MA 02172
Attn: Dr. Donald W. Oplinger 1

U. S. Army Missile Command
Redstone Scientific Information Center
Redstone Arsenal, AL 35808
Attn: Document Section 1

Commanding Officer
U. S. Army Research Office (Durham)
Box CM, Duke Station
Durham, NC 27706
Attn: Library 1

Director, Code 6180
U. S. Naval Research Lab.
Washington, DC 20390
Attn: Library 1

Bureau of Naval Weapons
Dept. of the Navy
Washington, DC 20360
Attn: RRRE-6 1

National Technical Information Service
Springfield, VA 22151 25

Naval Air Propulsion Center
P. O. Box 7176
Trenton, NJ 08628
Attn: James Salvino 1
Robert Delucia 1
G. J. Manganu 1

Federal Aviation Administration
Code ANE-214, Propulsion Section
12 New England Executive Park
Burlington, MA 01803
Attn: Robert Berman 1

Federal Aviation Administration
AFS-140
Washington, DC 20591
Attn: A. K. Forney 1

FAA, AFS-140
800 Independence Ave., SW
Washington, DC 20591
Attn: Dr. Thomas G. Horeff 1

FAA, AFS-520
2100 Second Street, SW
Washington, DC 20591
Attn: Cdr. John J. Shea 1

National Transportation Safety Board
800 Independence Ave., SW
Washington, DC 20594
Attn: Edward P. Wizniak, TE-20 1

MIT
Cambridge, MA 02139
Attn: Prof. John Dugundji (Room 33-313) 1
Prof. James Mar (Room 33-313) 1
Prof. Rene H. Miller (Room 33-207) 1
Prof. Emmett A. Witmer (Room 41-219) 1
Dr. David Roylance (Room 6-202) 1

Detroit Diesel Allison
General Motor Co.
Indianapolis, IN 46206
Attn: Library 1
Dr. Pete Tram 1
Dr. Lynn Snyder 1
R. Jay 1
L. Burns 1

AVCO, Lycoming Division
550 South Main Street
Stratford, CT 06497
Attn: Library 1

Beech Aircraft Corp., Plant 1
Wichita, KS 67201
Attn: M. K. O'Connor 1

Boeing Commercial Airplane Co.
Seattle, WA 98111
Attn: Library 1

Boeing Aerospace Company
P. O. Box 3999
Seattle, WA 98124
Attn: Library 1

McDonnel Douglas Aircraft Co.
P.O. Box 516
Lambert Field, MO 63166
Attn: Library 1

Douglas Aircraft Co.
3855 Lakewood Blvd.
Long Beach, CA 90846
Attn: Library 1

General Dynamics/Convair Aerospace
P.O. Box 1128
San Diego, CA 92112
Attn: Library 1

Grumman Aircraft Engineering Corp.
Bethpage, Long Island, NY 11714
Attn: Library 1

General Electric Company
Building 53, Room 332
One River Road
Schenectady, NY 12345
Attn: Dr. Kemal Arin

Texas A & M University
Dept. of Mechanical Engineering
College Station, TX 77843-3123
Attn: Professor Dara Childs
Turbomachinery Laboratories

Massachusetts Institute of Technology
Department of Aero. and Astro.
Gas Turbine & Plasma Dynamics Lab
Cambridge, MA 02139
Attn: Professor Edward F. Crawley

Arnold Eng Dev Center/Sverdrup
Tullahoma, TN
Attn: Mr. Tom Cromer

Hamilton Standard Division
United Technologies Corporation
Windsor Locks, CT 06096
Attn: Mr. Allen Dale

Rockwell International
Rockettdyne Division
6603 Canoga Avenue
Canoga Park, CA 91304
Attn: Mr. Gary Davis

Williams International
2280 West Maple Road
P.O. Box 200
Walled Lake, MI 48088
Attn: Mr. Gary Ernst

Pratt & Whitney Aircraft Group
Government Products Division
West Palm Beach, FL
Attn: Mr. Tom Farmer

Allison Gas Turbine Division
General Motors Corporation
Indianapolis Operation, P.O. Box 420
Indianapolis, IN 46206-0420
Attn: Mr. Allen Fox

General Dynamics/Electric Boat Division
Department 443
Applied Mechanics Section
Groton, CT 06340
Attn: Mr. Steve Gordon

Pratt & Whitney Aircraft Group
Commercial Products Division, 163-09
400 Main Street
East Hartford, CT 06108
Attn: Mr. Dave Hibner

NASA Headquarters
Washington, DC 20546
Attn: Dr. Murray Hirschbein

Case Western Reserve University
Department of Civil Engineering
Cleveland, OH 44106
Attn: Professor Arthur Huckelbridge

Wright-Patterson Air Force Base
AFWAL/MLLN
Dayton, OH 45433
Attn: Dr. D.I.G. Jones

Boeing Commercial Airplane Company
Prop - B8405 - 180 - 318
P.O. Box 3707
Seattle, WA 98124
Attn: Mr. C. M. Lewis, Jr.

Renesselaer Polytechnic Institute
Dept. of Mech. and Aero. Eng.
Troy, NY 12181
Attn: Professor Bob Loewy

Garrett Turbine Engine Company
111 South 34th Street
P.O. Box 5217
Phoenix, AZ 85010
Attn: Mr. Lee Matsch

NASA Marshall Space Flight Center
MS EE 51
Huntsville, AL 35812
Attn: Mr. John Moorehead